ELSEVIER

Contents lists available at ScienceDirect

Applied Catalysis A, General

journal homepage: www.elsevier.com/locate/apcata





Syngas to sustainable aviation fuel: Emerging catalysts and routes

Evert Boymans^a, Yadolah Ganjkhanlou^{a,*}, Iker Agirrezabal-Telleria^{b,*}, Nerea Viar^b, Berend Vreugdenhil^a

- ^a Energy Transition Unit, Netherlands Organization for Applied Scientific Research (TNO), Petten 1755 LE, the Netherlands
- b Department of Chemical and Environmental Engineering of the Bilbao Engineering School, University of Basque Country (UPV/EHU), Plaza Torres Quevedo 1, Bilbao 48013, Spain

ARTICLE INFO

Keywords: Sustainable aviation fuel Syngas Olefin Methanol Bifunctional Catalyst Alcohol

ABSTRACT

As the aviation sector needs to decarbonize, sustainable aviation fuel produced from syngas offers a promising pathway to decrease CO_2 emissions. A wide range of carbon sources including biomass, CO_2 , and municipal and plastic waste can be used as sustainable feedstock to produce syngas. This review provides a comprehensive overview of all known routes for converting syngas into jet-range hydrocarbons, with particular emphasis on emerging catalytic approaches at low technology readiness levels. These include direct syngas-to-jet fuel range hydrocarbons (HCs) and syngas-to-olefins-to-jet fuel range HCs as well as routes with methanol- or ethanol as intermediate. We assess recent advances in catalyst design, such as bifunctional, core–shell, and tandem systems, and discuss how these compare to established pathways like Fischer–Tropsch synthesis, which is already certified under ASTM D7566. By benchmarking emerging technologies against ASTM-certified and near-commercial processes, this review identifies key opportunities and technical challenges that must be addressed to accelerate the deployment of syngas-based SAF solutions.

1. Introduction

While electrification is expected to play a central role in reducing CO_2 emissions across the transport sector, it remains unfeasible for aviation due to the high energy density requirements of air travel. Additionally, commercial aircrafts have average lifespans of over 30 years which means planes built today are likely to remain in operation until around 2055. In this context, Sustainable Aviation Fuel (SAF) emerges as a critical solution. SAF refers to drop-in liquid fuels produced from renewable or waste-based feedstocks that are fully compatible with existing jet engines and fuel infrastructure. Depending on the chosen feedstock and conversion pathway, SAF can achieve an up to 80 % reduction in lifecycle CO_2 emissions compared to conventional jet fuel [11].

Policy instruments like the European Union's ReFuelEU Aviation initiative and the ICAO's CORSIA program are driving SAF adoption through blending mandates and carbon accounting mechanisms. These frameworks have created both regulatory and market incentives to expand SAF production as part of the aviation sector's pathway to netzero emissions by 2050.

To date, the vast majority of commercial SAF is produced in the form

of Hydroprocessed Esters and Fatty Acids (HEFA) [2,3]. HEFA uses waste oils, animal fats, and other lipid-based feedstocks, converting them via hydrotreatment into jet fuel-range hydrocarbons (HCs). It is the most technologically mature and widely adopted SAF pathway, owing to its relatively low production cost, high compatibility with fossil fuel infrastructure, and established regulatory status.

In addition to HEFA, biofuels like biodiesel and SAF can be produced from biomass via several alternative pathways. Key processes include the transesterification of vegetable oils or animal fats to produce fatty acid methyl esters (FAME, alternative to diesel), the gasification of organic residues to generate syngas followed by either Fischer–Tropsch synthesis (FTS) or methanol synthesis with subsequent conversion to jet fuel, as well as hydrothermal liquefaction. Another notable route involves the fermentation of biomass to produce alcohol, such as isobutanol, which are then upgraded to SAF through alcohol-to-jet (ATJ) technologies. Transesterification and HEFA require lipid feedstocks and involve only one or two conversion steps, making them more commercially mature. There are over 200 FAME production facilities in the EU [4]. Production has increasingly shifted from FAME to HEFA due to the use of waste oils and fats, which qualify for double counting under EU mandates. In 2020, EU biodiesel production was 15,955 ML, including

E-mail addresses: yadi.ganjkhanlou@tno.nl (Y. Ganjkhanlou), iker.aguirrezabal@ehu.eus (I. Agirrezabal-Telleria).

^{*} Corresponding authors.

3412 ML of hydrotreated vegetable oil [5].

The primary limitation of the HEFA pathway for SAF production is the constrained availability of suitable lipid-based feedstocks, particularly used cooking oil (UCO). In the European Union, demand for UCO already far exceeds domestic collection capacity. Europe consumes approximately 130,000 barrels of UCO daily, eight times more than it collects locally [6]. This shortfall has driven heavy reliance on imports, especially from China. However, recent trade developments have added further strain to the supply chain. In April 2025, the United States imposed a 125% import tariff on Chinese UCO, halting exports to its largest market [7]. In response, Chinese exporters redirected shipments toward Europe and other Asian countries [7]. While this has temporarily increased European supply, experts warn that global UCO demand is projected to triple by 2030, potentially surpassing the sustainable collection capacity even in major producing countries like China [6]. These trends underscore that HEFA-based SAF, while mature and technically viable, is not scalable at the levels required for widespread decarbonization of aviation. Alternative feedstocks and routes, such as Fischer-Tropsch, methanol-to-jet, and Power-to-Liquid, must be advanced to ensure long-term supply resilience.

However, the biomass-to-liquid (BTL) route via FTS, and syngas conversion more broadly, remains less developed, primarily due to high process complexity and significant upfront capital investment. Unlike HEFA or FAME, BTL involves multiple steps: from solid feedstock to gas and finally to liquid (Fig. 1). Its main advantage is broader feedstock availability, including forest residues, energy crops, and municipal waste. As fossil fuel prices rise and SAF incentives grow, BTL may become more competitive, especially when using advanced feedstocks

that enable double counting. On the other hand, syngas routes have the advantage of using diverse (including bio-based lignocellulosic) feedstocks as summarized in Fig. 1. Advantages are that feedstocks are not limited to biomass itself, but waste (not only organic waste but also plastic waste) as well as fossil fuel-based sources (coal and natural gas) can be used. Even CO_2 and renewable hydrogen after reverse water gas shift (rev-WGS) can be used to obtain syngas and then aviation fuels known as eSAF.

2. SAF Certification Under ASTM D7566

The technical certification of SAF is governed by ASTM D7566, which outlines approved synthetic fuel components and their blending limits with conventional jet fuel (ASTM D1655). Each pathway has specific annexes under D7566 as listed in Table 1. Table S1 in the supporting information lists the main ASTM specification limits for properties of Jet A-1 alongside representative values for Jet A-1, a 50 % SPK blend, and pure SPK, covering parameters such as cold-flow performance, density, aromatic content, and other key operational properties. It is important to note that the specification requirements for SAF differ from those for conventional fossil-derived jet fuels, as SAF is not vet certified for use as a 100 % standalone fuel in current aviation practice. For instance, highly paraffinic FT-SPK product while meets smoke point and freeze point criteria under ASTM D1655 (Table S1), but its density is often at the lower end of the allowable range. Therefore, SAF must be blended, often up to a maximum of 50 vol% depending on the ASTM pathway (Table 1), with conventional jet fuel to meet ASTM D7566/ D1655 standards.

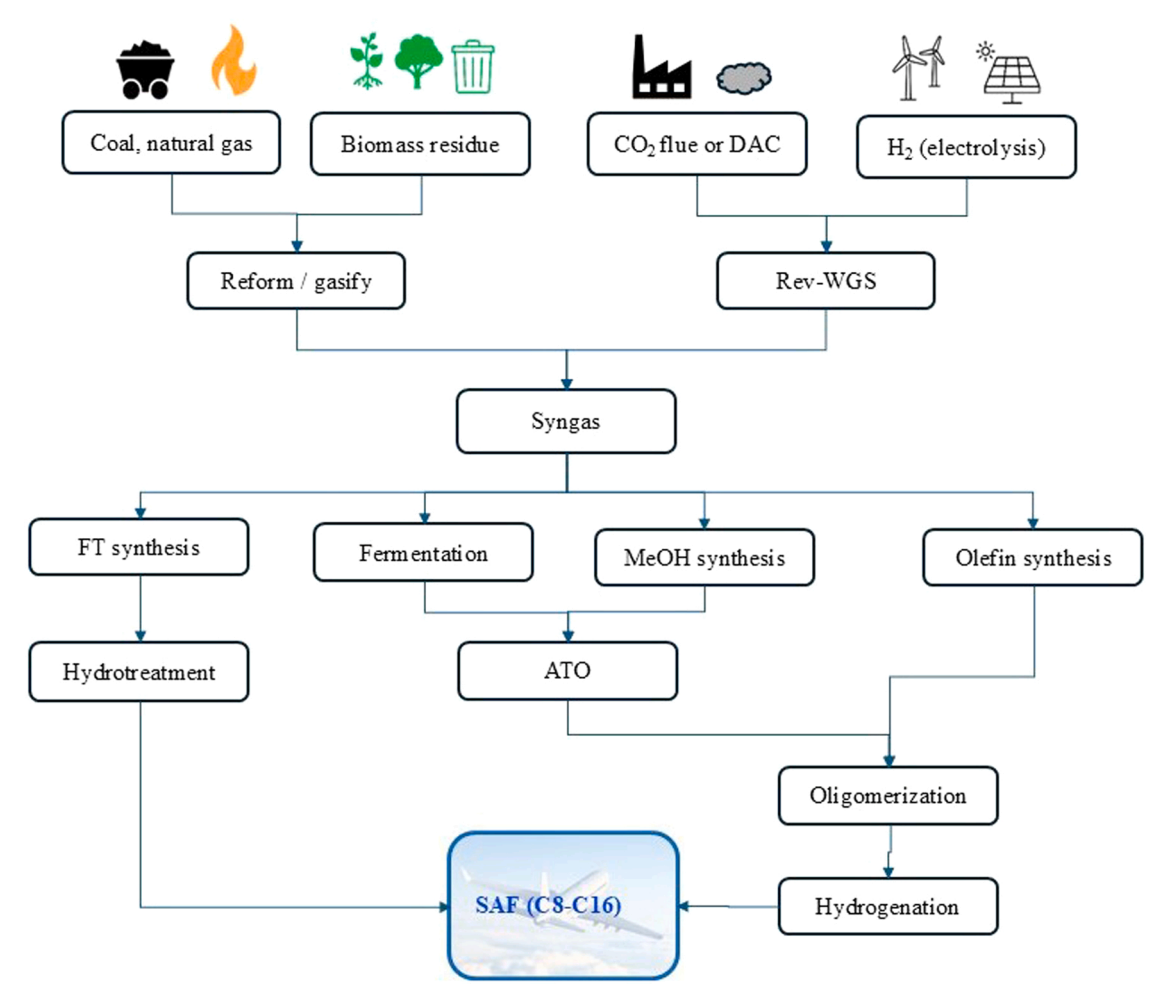


Fig. 1. syngas from different feedstocks can be converted to aviation fuels through different routes.

Table 1Overview of the ASTM D7566-23b annexes describing the different (biobased) processing routes.

Annex	Title	Product name	Manufacture	Max. Blending
A1	Fischer-tropsch hydroprocessed synthesized paraffinic kerosine	FT-SPK	Fischer-Tropsch (FT) process using Iron or Cobalt catalyst with subsequent hydroprocessing.	50 %
A2	Synthesized paraffinic kerosine from hydroprocessed esters and fatty acids	HEFA SPK	Hydrogenation and deoxygenation of fatty acid esters and free fatty acids with subsequent hydroprocessing.	50 %
A3	Synthesized iso-paraffins from hydroprocessed fermented sugars	SIP	Hydroprocessed synthesized iso-paraffins wholly derived from farnesene produced from fermentable sugars with subsequent hydroprocessing.	10 %
A4	Synthesized kerosine with aromatics derived by alkylation of light aromatics from non- petroleum sources	SPK/A	FT SPK as defined in Annex A1 combined with synthesized aromatics from the alkylation of non-petroleum derived light aromatics (primarily benzene) with subsequent hydroprocessing.	50 %
A5	Alcohol-to-jet synthetic paraffinic kerosene (atj-spk)	ATJ-SPK	Synthesized paraffinic kerosene wholly derived from either ethanol or isobutanol through oligomerization, hydrogenation, and fractionation.	50 %
A6	Synthesized kerosine from hydrothermal conversion of fatty acid esters and fatty acids	CHJ (Catalytic Hydrothermolysis Jet)	Hydrothermal conversion of fatty acid esters and free fatty acids with subsequent hydroprocessing.	50 %
A7	Synthesized paraffinic kerosine from hydroprocessed HCs, esters and fatty acids	HC-HEFA SPK	Paraffins derived from hydrogenation and deoxy-genation of bio-derived HCs (Botryococcus braunii species of algae), fatty acid esters, and free fatty acids.	10 %
A8	Alcohol-to-jet synthetic paraffinic kerosene with aromatics (atj-ska)	ATJ-SKA	Addition to ATJ-SPK of an aromatic product stream comprising dehydration, aromatization, hydrogenation, and fractionation.	50 %

This blending ensures that properties such as aromatic content, density, and seal-swelling capability are met by contributions from the fossil-derived portion of the blend. For example, aromatics, absent or very low in FT-derived SAF, are supplied by the conventional jet fuel fraction to maintain compatibility with existing elastomer seals in aircraft fuel systems. In commercial Jet A-1, aromatics typically range from ~15–23 % vol, while synthetic paraffinic kerosenes (SPKs) such as FT-SPK contain almost none. Cycloalkanes and aromatics in fossilderived jet fuel play an important role in improving cold-flow properties and volumetric energy density, while paraffinic components, especially iso-paraffins, enhance combustion quality and reduce soot formation (Aromatics though helpful for sealing and cold flow properties cause also soot formation and there is research ongoing to improve sealing without aromatic presence in jet fuels). As a result, FT-based SAF can be fully compliant when blended within the approved limits, delivering the sustainability benefits while relying on the conventional component to meet certain specification requirements.

Each pathway has a specified maximum blending ratio and must meet jet fuel specifications after blending. Among *syngas-based routes*, FT-SPK is currently the most directly applicable because it is the only ASTM-certified option (Annex A1) and follows a well-established two-step process: FTS to long-chain HCs, followed by hydrocracking and isomerization. After upgrading, typical cobalt-based FT processes yield roughly 25–45 % C_8 – C_{16} HCs depending on chain growth probability (α), with the remainder as lighter gases, naphtha-range fractions, and heavier waxes. In contrast, the other major syngas-derived pathway, via methanol (MtJ), is still pending ASTM approval. This makes FT-SPK the most straightforward candidate for transitioning from fossil-derived to renewable SAF, both in regulatory readiness and technical deployment.

There are, however, ASTM-approved SAF pathways in which aromatics are directly included in the finished fuel. These include FT-SPK/A (Annex A4) and catalytic hydrothermolysis jet (CHJ, Annex A6) [8]. FT-SPK/A was pioneered by Sasol and differs from FT-SPK by the addition of an aromatic fraction to meet density and seal-swelling requirements. However, these aromatics are not generated from the FTS product itself but are typically supplied from fossil-derived coal tar light naphtha streams (not petroleum based but still fossil based)[9]. In contrast, CHJ fuels inherently produce cycloalkanes and aromatics during hydrothermal upgrading of lipids, providing a higher-density SAF stream without reliance on fossil aromatic co-feeds. The existence of such pathways illustrates that ASTM D7566 certification regulates not only fuel properties but also the production route; even if a new SAF has identical composition to an approved fuel, it must undergo the ASTM D4054 approval process unless its pathway is already described in an annex.

In addition to aromatic content, ASTM D1655 specifies other critical fuel properties, including smoke point (\geq 25 mm for Jet A-1), freeze point (\leq –47 °C), and density (0.775–0.840 g·cm $^{-3}$ at 15 °C). Paraffinic SAF from FT-SPK, STO, and ATJ routes generally meet or exceed smoke point and freeze point requirements but often has a lower density than petroleum-derived fuels. Blending with aromatic- or cycloalkane-rich fractions (e.g., from CHJ, HEFA-SPK, or oligomerized aromatics) can adjust density to ASTM limits while retaining the clean-burning benefits of paraffinic HCs.

3. Scope of this Review

While HEFA remains the dominant pathway for SAF production today, future growth will require diversification of both feedstocks and conversion routes. Syngas-based pathways, including FTS and MtJ processes, offer promising alternatives. These technologies can utilize CO₂, renewable hydrogen, and solid waste, promoting circular carbon use and improved sustainability (Fig. 1). For instance, companies like LanzaJet produce alcohol from syngas via fermentation, which can then be upgraded through alcohol-to-jet (AtJ) processes. However, this review focuses primarily on chemical conversion routes, with an emphasis on catalytic developments. Biochemical routes such as fermentation are not covered in detail, as they fall outside the scope of this work. Similarly, reactor intensification strategies, particularly for low-temperature FTS, are not discussed here, as they have been addressed in our recent review [10] and other publications [11,1,2].

This review compares various syngas-based pathways and focuses on:

- Commercial and near-commercial routes, such as FTS and its ASTM-certified variants (e.g., FT-SPK, FT-SPK/A), discussing their limitations in jet-range selectivity and opportunities for process optimization.
- Direct syngas-to-jet (STJ) pathways, where bifunctional or core-shell catalysts integrate syngas conversion and hydro-upgrading steps in a single reactor system to enhance jet-fuel selectivity.
- Syngas-to-olefins-to-jet (STO) processes, involving olefin synthesis followed by oligomerization and hydrogenation to produce C8–C16 HCs with improved carbon efficiency.
- Emerging near-commercial MtJ processes that are pending ASTM certification, along with recent advancements in catalyst development and process integration. This includes both MtJ and ethanolbased routes, featuring two- and three-step catalytic sequences that convert syngas-derived alcohols into jet-range fuels.
- Opportunities and barriers for SAF from renewable syngas.

The paper emphasizes strategies for improving jet-range HC selectivity (C₈-C₁₆) and scaling SAF production from smaller, decentralized feedstock sources such as biomass and municipal waste. Fig. 2 summarizes the commercial routes for converting syngas into jet fuel (excluding fermentation) and also shows the product selectivity at each step, as well as the overall selectivity to jet fuel. One can already see that, in general, the overall selectivity is around 60 % or lower for different routes, which indicates that there is still room for further improvement in selectivity. Here it should be noted that, requirements for jet fuel go beyond simply having HCs of certain carbon number, hydrocarbon in the range of C₈–C₁₆ already qualify the liquid fuels for many (though not all) of the jet fuels requirements (see FT-SPK in the SI, for instance). The remaining properties (e.g., cold flow properties, density and sealing properties) can be achieved through blending. Therefore, the C₈–C₁₆ fraction of products is often referred to as jet-fuel-range HCs [13-15], although additional blending is typically required for these products to fully meet the specifications of commercial jet fuels, as discussed in the previous section. In this review, we primarily focused on syngas conversion routes that yield HCs in this range, while also considering, where possible, whether aromatic, cycloalkanes and isomers are formed in the product. It should be noted that full specification of products usually needs scale-up of the process and is not relevant for early stage catalyst/route development where liquid production is usually limited to a few milliliters.

While other HCs produced can also be used for various purposes and in current fossil fuel-based systems, such as FT reactors, co-products contribute to profitability. In the future, the demand for other liquid fuels is expected to decline due to the ongoing electrification of other sectors. Therefore, achieving higher selectivity toward jet fuel will become more desirable, especially as SAF production becomes more decentralized to match the local availability of feedstocks. In the future, as the allowable blending ratio of SAF increases, the fuel itself will need to fully meet jet fuel specifications. To address this, De Klerk proposed the concept of FT-SPK/A [9], in which aromatics are introduced so that FT-based fuels can directly satisfy jet fuel requirements. Those aromatics, and if necessary cyclic hydrocarbons, can be produced by alternative sustainable routes such as lignin valorization, catalytic fast pyrolysis of biomass, alcohol and olefin-to-aromatics conversion (e.g., over H-ZSM-5 or Zn-ZSM5), or dehydrocyclization of bio-naphtha (as mentioned, this would also require the establishment of a new annex under the ASTM D7566 standard for certification).

4. SAF from syngas

4.1. Fischer-Tropsch-based SAF

FTS is a thermochemical process that converts syngas, a mixture of CO, H_2 , and CO_2 , into HCs. Syngas can be produced from various feed-stocks: biomass, municipal solid waste, industrial off-gases, or renewable electricity plus captured CO_2 .

As mentioned in the previous section, FTS is already ASTM-certified (FT-SPK, FT-SPK/A- ASTM D7566), and commercially applied in fossil-based plants:

- Shell's SMDS and Pearl GTL plants (Malaysia, Qatar) use natural gas and cobalt-based LTFT in fixed-bed reactors [16].
- Sasol's Secunda plant (South Africa), a legacy coal-to-liquid facility, applies HTFT and is the world's largest GHG point source [17].
- ORYX GTL in Qatar, a joint venture with Sasol, uses slurry-phase LTFT.

LTFT operates at 200–250 °C in wall-cooled fixed or slurry bed reactors. It produces a high concentration of heavy paraffins (C22 +), which are then hydrocracked and isomerized into jet-range fuels. Shell's SMDS process achieves a product split of roughly 25 % naphtha, 50 % kerosene, and 25 % diesel [16]. With 90 % C5 + selectivity, this equates to \sim 45 % jet fuel yield. Refinery modifications can raise this to 63 % [18].

However, these commercial setups are not optimized for SAF. Their product distributions follow the Anderson–Schulz–Flory (ASF) model, which yields a wide carbon range. For smaller, bio-based facilities, focusing on jet-range HCs (C8–C16) is critical for process efficiency [19].

Some pilot efforts in Europe aim to demonstrate renewable syngasto-jet SAF:

- Sunfire-Atmosfair (Germany) uses renewable electricity, water, and CO₂ to generate syngas for FT synthesis [20].
- **BioTfueL (France)** targets FT-SAF from thermochemically converted biomass [21].

The main commercial catalysts used in these FTS processes are typically cobalt-based catalysts (e.g., Co/Al₂O₃ or Co/SiO₂) or iron-based catalysts (e.g., Fe–Cu–K) though for jet fuel production low temperature

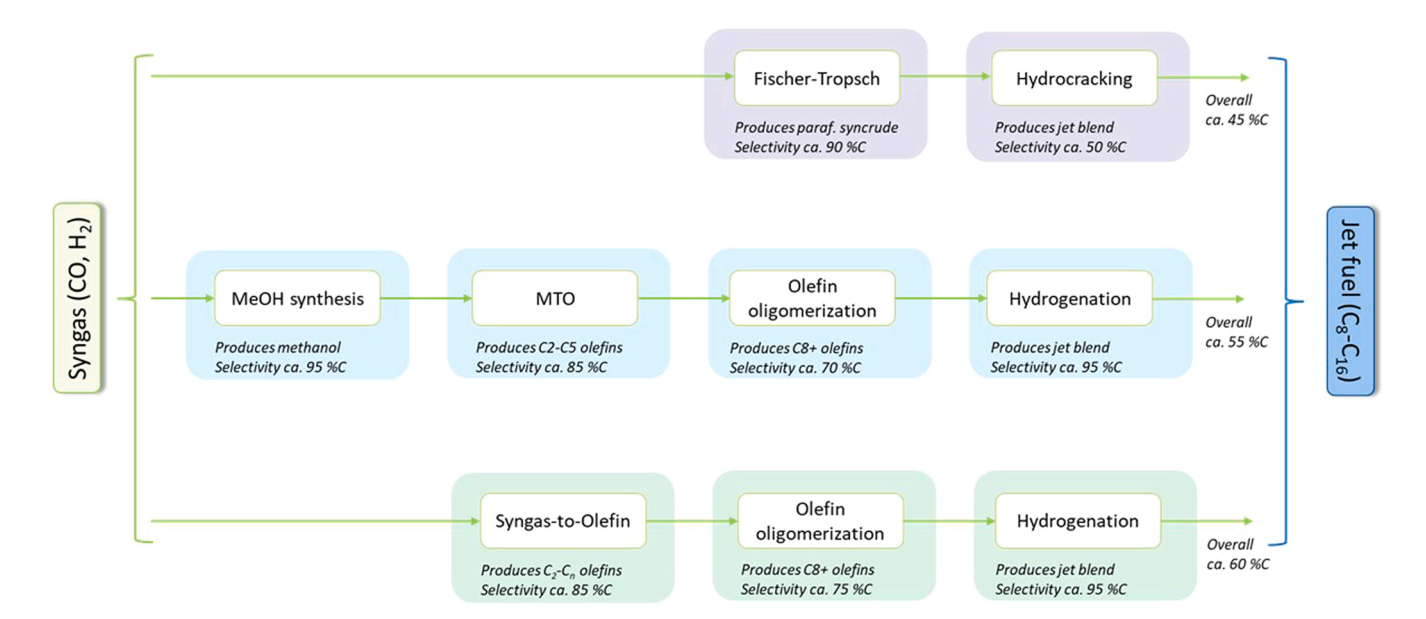


Fig. 2. current commercial or near commercial routes to convert syngas to jet fuel (note that the estimated selectivity is for industrial processes and tailored processes and novel routes may have different selectivity's).

FTS is preferred due to higher selectivity to SAF (e.g. Shell's SMDS and Pearl GTL). Co-based catalysts under LTFT conditions offer high activity and long lifetimes. Iron catalysts are more tolerant of CO₂-rich syngas but less selective for heavy products. Also, their activity in WGS may come at the price of converting CO to CO₂ in CO rich syngas, which is not desired. As mentioned, to shift the product range toward kerosene, downstream hydrotreatment is applied specially in case of LTFT, including hydrocracking and hydroisomerization [16,22,23].

Some of the promising catalysts and reactor designs in this field to produce more fuel are:

- **Bifunctional catalysts** (e.g., Co supported on zeolites) that integrate FT and cracking [14,24,25].
- **Core-shell structures** for shape-selective catalysis [26,27].
- Microchannel and modular reactors for improved heat control and decentralized production [28–30].

Jet A-1 fuel specifications set limits for boiling point, density, and freezing point, typically requiring branched paraffins in the C8–C16 range. Linear alkanes (common in FT products) are not ideal due to their poor cold flow properties.

Shell's "ideal hydrocracking" approach selectively cracks heavier molecules to maximize kerosene while minimizing gas or light fractions [22]. According to de Klerk, this can push kerosene selectivity up to \sim 63 % [9,18].

4.2. Direct Syngas-to-Jet (STJ)

In the direct STJ approach, the conventional FTS process is simplified by integrating the synthesis and upgrading steps into a single catalytic system. This concept aims to circumvent the limitations of the ASF distribution, which naturally favors a wide product range and necessitates downstream hydrocracking and separation. By employing bifunctional or multifunctional catalysts which combine an FTS-active phase (e.g., Fe, Co, Ni, or Ru) with components active for hydrotreatment (e.g., hydrocracking, hydroisomerization) or oligomerization, allowing deviation from ASF distribution and enabling more direct production of jetrange HCs. Direct STJ routes can potentially improve jet fuel selectivity, simplify processing, and reduce overall costs [36,37].

Several catalyst configurations have been developed to enable this integration:

- Dual-bed systems separate the FTS and hydroprocessing zones physically within the reactor. This prevents the migration of promoter species (e.g., alkali metals) that may deactivate acidic sites in zeolites. However, this configuration may limit the synergistic interaction between the two functionalities, often resulting in reduced product branching and a broader product distribution [25].
- Physically mixed catalysts provide intimate contact between FTS-active metals (such as Co or Fe) and acidic supports like zeolites.
 While this configuration has demonstrated increased CO conversion and enhanced C5–C11 selectivity, it also leads to higher methane and light gas production, likely due to local hot spots and enhanced hydrogenolysis reactions [31]. Nonetheless, physical mixing often outperforms dual-bed systems in terms of branching and mid-range product selectivity.
- Core-shell catalysts encapsulate an FTS-active core (e.g., Co or Fe) within a porous shell composed of hydroprocessing materials such as zeolites. This architecture provides shape selectivity, confinement effects, and controlled diffusion, enabling higher selectivity to isoparaffins. Examples include Co/Al₂O₃@H-Beta, Ru-CO@CeO₂ and Co@SiO₂ systems, which demonstrated peaked product distributions around C₅−C₁₂ [26,32,33]. Pore size of the shell layer is the main factor affecting product distribution. Main challenges of this approach are the complex synthesis procedures, possible diffusional limitations of CO but also product, and the unknown long-term

stability of the catalysts [25]. Also, isomerization is severe and sometime more than what is needed in jet fuels. Confined Co particles in silica (structure like watermelon) are also reported to have enhanced liquid fuel production [43] and in this case, controlled diffusion/mass transfer of CO and product is the main reason for the enhancement of liquid fuel production since the silica layer is not active in hydroisomerization.

• Bifunctional catalysts are typically prepared by dispersing FTS-active metals directly onto mesoporous zeolites or acidic oxides. Mesoporosity is essential to accommodate larger metal clusters, enhance diffusion, and maintain catalytic activity. Acidity tuning via desilication (alkaline treatment) and dealumination (acidic treatment) is also crucial, as only zeolites with strong acid sites show effective hydrocracking under LTFT conditions [14,25,34]. Cobalt-loaded mesoporous ZSM-5 and Beta zeolites have shown gasoline range selectivities exceeding 60 %, with no wax formation and reduced methane production compared to Co/SiO₂ [35].

An interesting extra benefit of STJ is that having zeolitic structures close to FT active phase not only performs hydrocracking of heavy species and improves the carbon distribution toward SAF, but also that many of zeolitic structures, such as ZSM-5, BEA and FAU(Y), are active in aromatization and can therefore increase the aromatic component in the product. In this way, they can outperform FT-SPK, which results in an almost aromatic free fuel (note that the aromatic presence is required in jet fuels as shown in Table S1 of the SI) [36] Hydroisomerization is also a side reaction that occur on the zeolite and in general zeolitic structure increase the branching of product which is also required in jet fuel (Table S1-typical ratio iso/n = 2)

Tsubaki's group has led several efforts in this area, showing that the zeolite structure and pore size strongly influence product distribution. While small-pore ZSM-5 promotes gasoline-range HCs, large-pore Beta and Y-type zeolites are better suited for producing C₈-C₁₆ jet fuel-range HCs [14,34,37,38]. For instance, Co/mesoY-La catalysts achieved up to 72 % selectivity toward jet fuel, benefiting from moderate Brønsted acidity and high mesoporosity. The ion exchange with La^{3 +} was shown to prevent excessive cracking and help achieve a high iso-/n-paraffin ratio, improving cold flow properties and fuel quality [14]. Having a promoter in the zeolite, such as Pt, which is active in hydrogenation, ensures that olefins are not present in the final product but it is also expected to hydrogenate part of formed aromatics, prevent coke formation, and avoid extra chain growth. In this regard, while not reported to the best of our knowledge, having Zn and Ga containing ZSM-5 (and other similar frameworks), which are active in aromatization[39], can increase the aromatic content in the final product.

Additional approaches involve co-feeding of 1-olefins (e.g., 1-octene, 1-decene) during FTS to promote chain growth via secondary insertion mechanisms. This strategy leads to significant deviation from ASF behavior and can increase the jet fuel selectivity above 65 %[13]. Re-adsorption and chain propagation of alpha-olefins on the surface were proposed to enhance the C8–C16 fraction [40–42]. Tsubaki's pilot-scale BTL plant employing this strategy achieved jet fuel production rates over 700 g·kg.cat $^{-1}$ ·h $^{-1}$ [19].

Despite these advancements, challenges remain regarding catalyst deactivation, coke formation, scalability, and unknown long-term performance of these systems. Moreover, some of the best-performing bifunctional systems rely on rare or expensive elements (e.g. Ru), which could hinder commercialization. Table 2 lists the CO conversion and selectivity of several bifunctional catalysts which are designed for SAF or other relevant fuel production.

4.3. Syngas-to-Olefins(-to-Jet)

An overview of the different pathways is shown in Fig. 1, and the typical selectivities achievable by each route are shown in Fig. 2, which together serve as a roadmap for the following subsections. The STO

route followed by oligomerization and hydrogenation presents an alternative path to SAF, potentially offering higher carbon efficiency than traditional FTS (Fig. 2). This strategy involves converting syngas to light olefins (C2–C4, also potentially heavy ones), which are then oligomerized to C8–C16 HCs and subsequently hydrogenated to produce paraffinic jet fuels. The overall process allows for more targeted carbon chain growth, reduced wax formation, and improved control over fuel properties [48]. The advantage of this approach is that oligomerization and hydrogenation are necessary in other routes like AtJ as well. Therefore, when necessary, they can be combined.

4.3.1. Fischer-Tropsch to Olefins (FTO)

Fe-based catalysts dominate FTO research due to their high selectivity to olefins and oxygenates under HTFT (300–350 $^{\circ}$ C) conditions, well development of process and economical costs. In general, FTO catalysts have been rapidly evolving in the last two decades. Catalysts such as Fe–Mn–K on silica or MgO supports have shown enhanced

C2–C4 selectivity, particularly when the H_2 /CO ratio is optimized to 1–2 [48,49]. Sodium- and sulfur-promoted Fe catalysts supported on α -Al₂O₃ or carbon nanofibers (CNFs) have achieved up to 60 wt% selectivity to light olefins at high CO conversion, with low methane yields [50–52].

Alkali-promoted iron carbide catalysts are widely utilized in FTO processes due to their cost-effectiveness and adaptability to various syngas compositions. The active phase, typically iron carbide (Fe₅C₂), facilitates olefin production. Alkali metals like potassium (K) or sodium (Na) are added as promoters to enhance olefin selectivity and suppress methane formation. These promoters donate electrons to iron species, promoting CO dissociative adsorption while suppressing hydrogen adsorption. However, a significant challenge with iron-based catalysts is the potential formation of iron oxides instead of carbides under certain conditions. Iron oxides are active in the water-gas shift (WGS) reaction, leading to increased CO₂ production and reduced olefin selectivity. In general, iron based catalysts have high selectivity to CO₂ (>30 %) due to WGS activity; however, in few cases (Table 3), the CO₂ formation

Table 2
Summary of bifunctional catalyst for direct syngas to SAF conversion.*

Strategy	Catalyst Used	CO C (%)	C ₈ -C ₁₆ S (%)	T (°C)	P (bar)	H ₂ / CO or M	TOS (h)	By-products / Notes
Benchmark LTFT + hydrocracking (HCr)	Co(+Ru)/Al ₂ O ₃ (LTFT) + hydrocracking [9,43]	20–70	~37 % before HCr [24] ~45 % after HCr (up to 63 % with ideal HCr)	220–230	20–25	2.0	1000 +*	slurry/fixed-bed*, Paraffinic, low aromatics; C ₁ -C ₄ ~20 %, C ₂₁ ⁺ =11-24 % [24], 29 % [44]
HTFT	FeK[36]	75–80	30–40	330	20	1.87	400	> 70 % linear (reported for C6) No aromatics C_1 – C_4 ~35 % No wax
	Commercial iron based FT [44]	-	20–25 (16.9 diesel)	250–270	10	2	-	C1-C4 = 23–27 % Iso/total= 21 %
Dual-bed	FeK + ZSM-5 [36]	50–70	50 % gasoline	330	20	1.87	400	C_2 – C_4 \sim 35 %, C_1 < 10 %, C_{21}^+ < 1 % Aromatic 20–35 % depend on acidity
	Fe + Pt/ZSM - 5[44]	-	15–25 (14.6–21.1 diesel)	250–270	10	2	-	C1-C4 = 20-31 % Iso/total= 81-84 %
	Co + Pt/ZSM - 5 [44]	-	50-55 (47.5 diesel)	230	10	2.0	-	22 % isomer in C10-C20
	Co + Pt/Beta [44]	-	40-45 (37.9 diesel)	230	10	2.0	-	42.7 % isomer in C10-C20
Physically mixed	Co + Pt/ZSM - 5 [44]	-	35–40 (33.2 diesel)	230	10	2.0	-	Increased C1-C4 comparing to baseline + 2 %, 41 % isomer C10-C20
	FeK + ZSM-5 [36]	75- > 50	29*gasoline	330	20	1.87	100 (before partial deactivation)	deactivation of catalyst Higher C ₁ (25–45 %); some aromatics expected
	Fe/Cu/La/Si + HZSM-5 [45]	75.3	24(mol)	290	17	1	83–90	74 % C1-C4 (slight increase of CH_4 comparing to their baseline) Iso/n = 1.5
	Co/Al ₂ O ₃ -Ni/ZSM-5/ γ-Al ₂ O ₃ [46]	85.9	40	230	10	2	_	40 % C1-C4 about 20 % increase to their baseline, C21 + less than 5 % comparing to 30 % without γ -Al ₂ O ₃ Iso/total > 80 %
Core-shell / confined	Co/Al ₂ O ₃ @H-Beta [26]	74	32	260	10	2	_	Less CH4 from both baseline and PM Iso/n = 2.34
	Ru-Co@CeO ₂ [32]	90	70	245	17.5	2	192	Ru boost jet selectivity comparing to their Ru free cat (no data on isomerization)
	Co@SiO ₂ [33]	85	30	260	10	2	n.r.	Iso/n = 1.88 $High C1: 44 % compared to 26–28 %$ of Co/SiO ₂
	Confined Co/SiO ₂ [47]	80	63-65*	220	20	2	_	No data on isomerization
Bifunctional	Co/mesoY–La [21]	70	72 (50 % gasoline)	250	20	1.0	10 h	Iso/n = 3.3 comparing to 0.6 reported for their baseline (Co/SiO ₂) C1-C4 = 14 % same as baseline, no wax while 21 % wax for Co/SiO ₂
Co-feeding 1-olefins	Co/ZrO ₂ –SiO ₂ bimodal [35] Slurry reactor	50 %	77.5 %	240	10	2	_	Wax while 21 % wax for Co/SiO ₂ Baseline= 29.0 % C8-C16. C1 also decreased from 19 % to below 5 % (olefin same/less than base)

^{* -}for these cases the selectivity is not directly reported in the mentioned references, and we estimated the selectivity based on the product distribution provided. $M = (H_2 - CO_2)/(CO + CO_2)$, Gas Hourly Space Velocity (GHSV) = 3000–12000 mL $g_{cal}^{-1}h^{-1}$ for majority of these reactions, C=conversion, S=selectivity, $C_n^{=}$:olefin with C number of n, LTFT: low temperature Fischer Tropsch, HTFT: High temperature Fischer Trospch, TOS: Time on Stream.

suppressed to below 25 % mainly by avoiding iron oxide phases and alkali promotion in the catalyst. Alkali promotion (for instance Na) can improve olefin selectivity but also increases WGS activity (see Table 3). Trade off here is to achieve sufficient olefin selectivity while suppressing CO₂, methane, and alkane formation.

Recently, Na–Ru/SiO₂ catalysts were shown to suppress methanation and the water-gas shift reaction while achieving > 80 % olefin selectivity at low CO₂ and CH₄ levels [53]. The catalyst performance is sensitive to the Ru nanoparticle size and Na/Ru ratio, offering a tunable platform for olefin production [48]. While it does not follow ASF distribution, this is quite similar to alkali promoted FTO catalysts (Fe- or Co-based). However, it is shown to be more selective, and Ru is generally the least active in WGS, leading to lower CO2 formation. More recently, sodium-promoted Ru/TiO2 catalysts have demonstrated the ability to tune the product distribution in FTO reactions by manipulating the dominant reaction mechanism. Sodium alters CO adsorption and activation, enabling a shift from the classical carbide mechanism, typically favoring C₅⁺ alkanes, to a CO insertion pathway that enhances olefin selectivity though in Ref. [48], suppression of extra hydrogenation is also mentioned as a reason for high olefin selectivity. By optimizing the sodium loading, a balanced catalytic system can be achieved, promoting efficient C-C coupling and long-chain olefin formation. Notably, the 0.5NaRu/TiO₂ catalyst exhibited a C₅⁺⁼ selectivity of 64.8 % with high space-time yield at 260 $^{\circ}$ C. While these studies offer critical mechanistic insights, less attention has been given to potential side reactions, such as the formation of oxygenated byproducts which can be problematic for downstream oligomerization step. However, certain downstream oligomerization and hydrogenation catalysts are capable of processing these intermediates (at least in low concentration <4 %), making their presence less problematic for overall SAF production [54].

Carbon-supported catalysts have also gained attention. Fe–Mn catalysts on nitrogen-doped carbon or reduced graphene oxide (rGO) have shown high activity and olefin yields, particularly when the Mn/Fe ratio is optimized to balance activity and olefin/paraffin ratios [55–57]. Zhu et al. recently developed Co–MnOx catalysts supported on glucose-derived carbon frameworks for selective long-chain α -olefin synthesis via FTS, showing promising results for downstream SAF conversion [58].

Cobalt carbide catalysts, particularly those based on Co_2C nanoprisms, have emerged as promising alternatives for direct syngas-to-olefins conversion. These catalysts exhibit high selectivity towards lower olefins (C_2 – C_4) and low methane formation under mild reaction conditions. The unique structure of Co_2C nanoprisms, with preferentially exposed {101} and {020} facets, plays a pivotal role in favoring olefin production and inhibiting methane formation [59]. Cobalt-based catalysts generally offer higher stability, less WGS (not always) and longer lifespans compared to Fe based ones, making them attractive for industrial applications. Core-shell structures have also been applied to improve FTO performance. Tsubaki's group demonstrated that Fe/SiO₂@silicalite-1 capsule catalysts can double the C_2 – C_4 olefin selectivity compared to conventional Fe/SiO₂, although diffusion limitations may reduce overall CO conversion [27,60].

4.3.2. Non-FTS Catalysts

To overcome ASF limitations and improve olefin selectivity, non-FTS catalytic systems have been developed. Jiao et al. [61] introduced a

Table 3
Different categories of supported olefin production catalysts from syngas

Type	Catalyst System	CO C (%)	Olefin S (%) C ₂ –C ₄ Ol.	T (°C)	P (bar)	H ₂ / CO	TOS (h)	By-products / CO₂ S.
Baseline FTO	Fe-Mn-K/SiO ₂ [48]	< 5	65 (C based without CO ₂)	300	2–5	1.5	n.r.	CH₄ 25 %, CO₂ ~n.r.
FTO	Fe/Al ₂ O ₃ [48]	5–20	41–49 (C based without CO ₂)	290	9	0.9	n.r.	CH ₄ 25 %, CO ₂ ~n.r. CO ₂ = 40-46 % for α - Al ₂ O ₃ [50] CO ₂ = 20 % for γ - Al ₂ O ₃ [50]
	Fe/SiO ₂ [48]	5	69	265	10	1.0	n.r.	$CH_4 = 21 \% CO_2 \sim n.r.$
	Fe/SiO ₂ [50]	50-100	56 (C based)	350	1	1.0	15	$CH_4 = 38 \%, CO_2 \sim n.r.$
	Ru/SiO ₂ [53]	75	18 (C ₂ =-C ₁₈ =)	260	10	2.0	50 +	CH_4 5–7 %, No CO_2 mainly C_2 - C_{18} alkanes
	Co/SiO ₂ [63]	32.5	7.7	230	10	2.0	n.r.	
Promoted FTO (Fe based)	Fe-Na-S/Al ₂ O ₃ [48]	80	53 % (C based without CO ₂)	340	20	1.0	60	CO conversion to $CO_2 \sim 50 \%$
	Fe-Na-S/CNF [48]	88	52 (C based without CO ₂)	330*	20*	1.0*	60	CO conversion to $CO_2 \sim 50 \%$
	Fe-Mn-K/Sil-2 [48]	90	70 (C based without CO ₂)	347	20	2.0	n.r.	$CH_4 = 22$, $CO_2 \sim n.r$.
	Fe-Mn/C [48]	n.r.	53	250	1	1.0	n.r.	$CH_4 = 11, CO_2 = 28$
	Cu-Fe-Mn [64]	96.9 %	40.1	300	20	2.0	80	CH ₄ = 20 %, CO ₂ = 23 %
Alkali-promoted Ru	Na-Ru/SiO ₂ [53]	45–70	80 (C ₂ =-C ₁₈ =)	260	10	2.0	500	$CH_4 < 4$ %, $CO_2 < 4$ %, linear HCs, oxygenate < 5 %
	Na–Ru/TiO₂ [54]	22	33.5 % Cs ⁺ in which 64.8 % ol.	260	20	2.0	110	$C_2 = -C_4 = \sim 19 \%$, CO_2 below detection
Promoted Co	Na(3 %)-Co/SiO ₂ [63]	2	42.9 (CO ₂ free)	250.	1	1.0	12	$CH_4 = 12.8 \%$, $CO_2 \sim n.r$.
	Co ₂ C nanoprisms [59]	6.3-25.3	31.9-60.8 (CO ₂ free)	250	1-10	0.5-2	30	CH ₄ = 3–5 %, CO ₂ = 46–49 %
OX-ZEO	CuZnAl + SAPO-34 [65]	20.4	53 (CO ₂ -free)	400	30	2.0	n.r.	Core–shell enhance C2-C4 however also increase C1, CO_2 = 49.5 %, CH_4 = 23.6 %
	$ZnCrO_{\times} + SAPO - 34$ [61]	17	80 (CO ₂ -free)	400	25	2.5	650	CO ₂ 41 %, CH ₄ = 2 %
	$ZnZrO_{\times} + SAPO - 34$	6.8	69 (CO ₂ -free)	400	10	2.0	200	CO ₂ 43 %, CH ₄ = 4.2 %
	Mn–Ga oxides + SAPO–34 [66]	19.5	68.3 (CO ₂ -free)	400	25	2.0	50	$CO_2 = 44$ %, $CH_4 = 10-15$ %
	ZrCeZnO×/SAPO-34 [67]	7–25.6	78.6–82 (CO ₂ -free)	400	10	2.0	5	CO ₂ = 45–48 %
	CrMnGa/SAPO-34 [68]	12–43.5	87.0 (CO ₂ -free)	400	30	2.0	n.r.	$CO_2 = 44-46 \%$

^{*} Typical GHSV = 1000-12000 mL $g_{cat}^{-1}h^{-1}$ for majority of these system, C=conversion, S=selectivity, $C_n^=$:olefin, OX–ZEO: mixed oxide-zeolite system, TOS: Time on Stream

mixed oxide/zeolite catalyst (ZnCrOx/MSAPO composite catalyst) that enables direct syngas conversion to light olefins via a tandem mechanism involving CO hydrogenation to methanol and subsequent dehydration and C–C coupling in SAPO zeolites. This catalyst achieved 74 % selectivity to C_2 – C_4 olefins, with CO_2 as the main by-product (41 %), indicating a pathway distinct from conventional FTS [61]. The system also displayed long-term stability over 110 h. Other tandem systems combining ZrZn oxides (for methanol synthesis) with SAPO-34 (for MTO reactions) also exhibit high olefin selectivity (~70 %), with the proximity of components enhancing interconversion and minimizing diffusion losses [62]. These approaches leverage the intermediate formation of methanol or DME, enabling better control over olefin distribution and reducing undesired by-products.

While mixed oxide combined with MTO catalysts are shown to be able to produce light olefins in a single step, a main limitation is the intrinsic WGS activity producing CO2 as a byproduct lowering the carbon conversion (CO2 selectivity is usually above 40 %). The two-step approach through methanol and MTO, despite requiring two distinct reactors, presently offers greater economic viability and selectivity as in this case methanol production is at low temperature around 200–250 °C and WGS is minimal. Table 3 lists the different catalysts (or composite catalyst) developed for olefin production from syngas. Based on this Table, we think that promoted FT active metals supported on different support (especially Ru one but also CO and promoted Fe and CO catalysts-Table 3) are more suitable for SAF production than mixed oxidezeolite systems as the WGS is much less than mixed oxide-zeolite system (CO₂ selectivity >40 % in most cases). This is due to their higher productivity (CO conversion > 50 % see for instance the Na-Ru based ones as well as Cu-Fe-Mn) and also the possibility of producing higher olefins and paraffins which are already in the SAF range HCs.

4.4. Recent development in Syngas-to- Methanol (-to-Jet)

Syngas conversion to methanol is well developed and already commercial. Methanol is therefore another intermediate for SAF production from syngas, in which either CO or CO_2 is converted with H_2 . In MtJ, methanol is first converted to dimethyl ether (DME), then oligomerized and hydrogenated into C8–C16 paraffinic HCs.

MtJ is not yet ASTM-approved, however it is in the ASTM pipeline for approval, and it is expected to be approved before 2030 [69]. Methanol is an attractive intermediate due to its production flexibility and existing market infrastructure. MtJ can be integrated into power-to-liquid schemes using CO2 and green hydrogen, as CO2-to-methanol conversion is more established, less energy-intensive, and typically more selective than direct CO2 conversion to oxygen-free HCs such as olefins. Nevertheless, MtJ still faces challenges in catalyst selectivity, oligomer control, and fuel certification. Typical selectivities for each step of MtJ are shown in Fig. 2. While the methanol-to-olefins (MTO) and hydrogenation steps are mature, industrialized technologies (TRL 9), the main bottleneck for scale-up remains the oligomerization stage [70] (selectivities up to 70 % is reported but this may also be further increased by recycling lighter olefins). Traditionally at a low TRL (3-4), oligomerization has recently advanced to TRL 5-6 in pilot-scale demonstrations by companies such as Metafuels [71] and in the EU Project TAKE-OFF [72]. Current approaches often employ a two-step sequence [70,72], starting with Ni-based metal catalysts to couple light olefins, followed by acidic solids such as zeolites or phosphoaluminosilicates to extend and refine the HC chain length. This step is essential for producing the desired C₈-C₁₆ jet-range fraction, yet heterogeneous oligomerization catalysts frequently induce excessive isomerization and branching, lowering density, affecting cold-flow properties, and yielding negligible aromatics. Arnold et al. [73,74] attempted co-oligomerization of C2-C4 olefins and achieved a high selectivity of 70 % in one step. The mentioned limitations make oligomerization the critical technical hurdle in bringing MtJ to full commercial deployment.

Methanol is one of the most commonly produced alcohols from

syngas through catalytic processes. The presence of a small amount of CO2 (typically less than 10%) in the syngas mixture can enhance methanol synthesis and help maintain optimal catalyst activity. A stoichiometric $(H_2 - CO_2)/(CO + CO_2)$ ratio of 2 is generally preferred to achieve high methanol yield [75] (due to thermodynamic of CO hydrogenation to methanol the one pass yield is below 60 % in fixed bed reactor [76]). Various metal catalysts, such as copper, zinc oxide, alumina, and magnesia, are commonly used in methanol production. The mostly developed industrial catalyst is Cu/ZnO/Al₂O₃ [76,77]. While methanol synthesis is a well-established commercial process, recent advancements have explored its further conversion into value-added products, including olefins via the methanol-to-olefins (MTO) process and SAF through subsequent catalytic upgrading. Also, catalytic developments are mostly focused to improve the catalyst for CO₂ hydrogenation to methanol rather than CO hydrogenation (see Table 4) but the main development in general is use of sorption enhanced [78-81], or membrane assisted reactor technology [82,83] which help to increase the one pass conversion above 80 %.

The industrial-scale production of SAF from methanol is gaining traction, with several companies working toward ASTM certification for their processes. One such company is *Topsoe*, which has proposed two distinct pathways for SAF production. The first involves producing methanol via the gasification of biomass, waste, tires, and plastic waste, which is then converted into advanced biofuel for aviation. The second pathway utilizes water electrolysis powered by renewable energy and CO_2 capture to synthesize methanol, which is subsequently upgraded into jet fuel. However, neither of these processes has yet received ASTM approval [84].

Another key player in the development of methanol-based SAF is *ExxonMobil*, which has advanced technologies for converting methanol into aviation fuel. Their primary focus is on the methanol-to-SAF process, but their technology is flexible enough to accommodate mixed alcohol feedstocks, providing additional versatility in sustainable fuel production [85].

In recent years, numerous patents have been published covering various aspects of the process. These patents reflect the ongoing efforts to enhance efficiency, scalability, and sustainability in the production of aviation fuels from methanol, reinforcing the potential of this approach as a viable alternative to conventional fossil-based fuels.

Among the patented technologies, *ExxonMobil* (2018) presents a method for converting methanol into aviation fuel using a reaction system composed of three reactors [86]. The first reactor dehydrates methanol (with 4 wt% water impurity) into dimethyl ether (DME) using acidic alumina as a catalyst. The DME and unreacted methanol enter a second conversion reactor operating at 400–530°C, 7–21 bar, and WHSV of $0.1–10~h^{-1}$, with a Zn- and P-modified zeolite catalyst. The products are separated into three streams: (1) aqueous phase, (2) naphtha-rich phase, and (3) a C₄ olefin- and paraffin-rich gaseous phase. The gaseous HCs are processed in a final oligomerization reactor at 125–250°C using an MRE or MFI zeolite catalyst. The output selectivity reaches 55–75 wt% of distillate fuel boiling range products, suitable for aviation fuel.

Another patented approach, developed by *Topsoe* in 2022 [87], introduces a two-stage reaction method for aviation fuel production. In the first stage, the methanol-to-olefins (MTO) conversion is performed by feeding a mixture of methanol and dimethyl ether (DME) and recycled light olefins into a reactor operating at relatively low pressures (1–15 bar) and high temperatures (300–360°C), using a zeolite modified with Mg and Ca. The water produced in the reaction is separated, and the resulting olefins are fed into a second reactor, where they mainly undergo dimerization or trimerization and are subsequently hydrogenated in the same unit. This integration reduces the number of stages required for SAF production, with the second reactor operating at higher pressures (20–40 bar) and lower temperatures (100–250°C) and employing a zeolite impregnated with a hydrogenating metal (Pd, Ru, Cu, Co, Ni,...). Though it is also mentioned that performing MTO in

Table 4 summary of catalyst syngas to methanol and methanol to olefin/SAF.

Method/ reaction	Step/sub-step	Catalyst System	Function / Notes	T (°C)	P (bar)	H ₂ / CO or M	TOS (h)	MeOH S and by products
Syngas to methanol catalyst	Syngas → Methanol	Cu/ZnO/Al ₂ O ₃ [98]	Industrial standard; sensitive to CO ₂	200–250	50–100	2.0	1000 +	S> 95 % CO ₂ < 3 % DME and other alcohols
Ž	$Syngas \rightarrow Methanol$	Cu/ZnO/MgO [99]	Improved stability and dispersion	200	70	1.7	180	S= 96-99 %
	$Syngas \rightarrow Methanol$	In₂O₃-based [100]	High activity for CO ₂ - rich syngas, less inhibition with H ₂ O	300	50	3	n.r.	S= >99 %
	$Syngas \rightarrow Methanol$	Cu/ZnO/ZrO ₂ [101] Productivity 8–9 mmol g _{cat} h ⁻¹	High activity for CO ₂ -rich syngas	240	40	2	n.r.	n.r.
	Syngas → Methanol	ZnO-ZrO ₂ + K [102]	Part of tandem system for methanol → ethanol pathway	310	50	1	20	n.r. for single cat.
MTO	MTP (Lurgi) [77] fixed bed	H-ZSM-5	72 % propylene, high TRL	450	~1.5	_	500-600	23 % C₅ ⁺ ; Aromatics, LPG
	MTO (UOP/INEOS) [77] fludized bed	H-SAPO-34	42 % propylene, 39 % ethylene, high TRL	350	2	_	n.r.	C ₅ ⁺ (5 %);
	MTO + water co- feeding [92]+ precoking	SAPO-34	Longer lifetime of catalyt, less coking	400	1	_	400–500	Improved C ₃ olefin
	MTO + coke to light olefins in second fluidized bed reactor [91]	SAPO-34	85% selectivity to olefins, CO, H_2 from regeneration	450	1	_	250	Low CO ₂
	Stable MTO → Zou et al. [93]	Ga-ZSM5	Ga improves stability;	400	1	_	180	ZSM5 alone deactivated in 10 min
ExxonMobil [86]— Methanol to	Methanol (96 %-rest H ₂ O) to DME	$\begin{array}{l} \gamma\text{-}Al_2O_3 \\ LHSV=1.66 \; h^{-1} \end{array}$	80 % conversion at 300 °C	n.r. expected: 250-400	Expected: 1–20	_	n.r.	DME and unreacted methanol
SAF	DME (unreacted MeOH)+recycled naphta → olefins	0.5–1.5 wt% Zn,P (P/ Z = 1.5–3molar)/zeolite (e.g. ZSM–5) Feed can also be: C - C4 alkyl group and / or other	WHSV= $0.1-10 \text{ h}^{-1}$	400–530	7–21	_	500/ \$MeOH -1 •gcat	Olefin/aromatic
	Olefins to gasoline range HCs	oxygenates MRE or MFI zeolite catalyst 1D,2D 10-member ring (e.g. ZSM5, ZSM–48)	Mainly C2-C3 olefin in feed	125–250	10–69	_	500 /g _{MeOH} ·g _{cat}	55–75 % fuel range HCs 35 % Ar 20 % Par. (C ₃ - C ₄ =50 %)
Topsoe patents MtJ[87] and oxygenate conversion [88]	Methanol/DME (recycled oxy.+ C2- C3 olefins) → olefins	zeolites with 1-D 10-ring (MRE, MTT and TON families) or 3D of MFI e.g. Mg- and Ca-ZSM5	Olefin production WHSV= 0.5 - $12~h^{-1}$ C= 50 - $100~\%$	320–480°C 400[77]	1–15 25 [77]	_	n.r.	25 % C ⁺ ₄ olefin selectivity low in aromatic (5–20 %) Light olefin in feed increase MTO cat lifetime
	Olefins → fuels (oligomerization + hydrogenation) stacked catalyst configuration	oligomerization catalyst: SPA, ion-ex. resins or zeolite: MRE, BEA, FAU, MTT, TON, MFI and MTW Hydrogenating metals (Pd, Rh, Ru, Pt, Ir, Re, Co, Cu, Ni, Mo, W containing catalyst) Preferably NiWS, Ni-Y, Ni-ZSM-23 also, Ni and Cu on alumina/ silica/titania/ZnO e.g.: Cu/ZnO/Al2O3	Hydrocarbon range shift WHSV= 0.5–6 h ⁻¹ mild hydrogenation condition	50-350 0-350[88]	20–40 1–100	_	n.r.	Tried to combine oligomerization and hydrogenation
NextChem [89,90]	MTO MTP	Zeolite/ silicoaluminophosphate	Fluidized bed; 400–420 °C; 2–2.5 barg	400–420	2–2.5	-	n.r.	C ₂ -C ₃ mainly 10–15 % Gasoline
Ellipe ed	$C_2/C_3 \rightarrow \text{butene}$	Modified ZSM-5 Bifunctional Ni catalyst on	0.5 and 6 h ⁻¹	50–200	10–70	_	n.r.	with 15–50 Ar) Mixture HCs fuels
	Butene \rightarrow fuel (for	zeolite/aluminosilicate H-zeolites/aluminosilicate,	$0.5 \ \mathrm{and} \ 4 \ \mathrm{h}^{-1}$	120–250	n.r.	_	n.r.	Ethylene C > 90 % Negligible aromatic
	MTP only this step)	MSA, M41S and in particular MCM-41 family, for example, or even FSM-16, HMS, SBA, MSI) and KIT-1						in this step with MSA
	hydrogenation	group VIII metals (e. g., Pt, Pd or Ni) supported on	WHSV 1-6 h ⁻¹	50–200	15–30		(Gasoline, jet fuel, diesel, and LPG. continued on next page)

Table 4 (continued)

Method/ reaction	Step/sub-step	Catalyst System	Function / Notes	T (°C)	P (bar)	H ₂ / CO or M	TOS (h)	MeOH S and by products
		conventional supports (e.g., activated carbon, alumina). trickle bed reactor						RON between 92 and 96; similarto the jet fuel

^{*} C: Conversion, S: Selectivity, weight hourly space velocity: WHSV, Par=Paraffin, Ar=aromatic, MSA=mesoporous Silica-Alumina, RON= research octane number.

higher pressure is beneficial as then no compression is needed between units.

Moreover, Topsoe further patented a three-reactor process that produces both propylene and sustainable aviation fuel [88]. In the first reactor, olefins are generated from methanol and DME with recycled propylene at pressures of 2-25 bar and temperatures of 240-360 °C, using phosphorus-modified (but also similarly Ca promoted) zeolites for enhanced stability. At the outlet, propylene is separated from the C₄–C₈ olefins. These C₄-C₈ olefins are then fed into a second reactor where they undergo oligomerization under conditions of 50-100 bar and 100-350 °C, employing catalysts such as zeolites, solid phosphoric acids (SPA), or ion exchange resins. Finally, in a third reactor, the oligomerized products are hydrogenated at 60-70 bar and 50-350 °C using a catalyst with hydrogenating metals such as Pd, Rh, Ru, or Pt to yield SAF. These two patents also propose the possibility of combining the oligomerization and hydrogenation steps into a single reactor, thereby simplifying the overall process. Main advantage of feeding olefin to MTO and using diluted oxygenate stream mentioned to be long lifetime of MTO catalyst.

Recently, NextChem patented a process for producing fuels from waste by converting olefins from methanol [89]. The process employs a fluidized-bed reactor followed by a two-stage reaction to produce a range of fuels. In the first stage, methanol containing 20 wt% water is fed into a fluidized-bed reactor that uses a zeolite or silicoaluminophosphate catalyst. Operating at relatively high temperatures (400–420 °C) and low pressures (2-2.5 barg), this reactor achieves nearly complete methanol conversion, yielding mainly water and HCs (predominantly C₂ and C₃). The water is condensed, and the gasoline fraction is separated by a de-hexanixer distillation column, accounting for 10-15 wt% of the HCs. The remaining HCs are then fed into a second reaction stage. Here, a bifunctional Ni catalyst supported on zeolites or mesoporous aluminosilicate materials is first employed to convert ethylene into butenes under conditions of 50–200 $^{\circ}$ C, 10–70 bar, and a WHSV of 0.5–6 h⁻¹. Subsequently, mesoporous aluminosilicates (in the absence of nickel) are used under similar operating conditions for oligomerization. The final product is a mixture of HCs that is separated into gasoline, jet fuel, diesel, and LPG. NextChem also patented similar process but specifically MTP [90] to produce fuel from it. It shares similar concepts except that it does not need first oligomerization of ethylene and directly oligomerize propylene with acid catalyst (e.g. mesoporous silica-alumina).

In addition to the innovations presented in the patents, recent research has focused on optimizing catalytic stability and selectivity toward desired products. Several studies have explored strategies to optimize the process by investigating coke deposition. Zhou et al. [91] developed an approach to improve the economics and sustainable viability of MTO process by converting coke generated during the reaction into light olefins. Through a steam cracking process over a SAPO-34 zeolite, they achieved a direct conversion of coke to light olefins with an 85 % selectivity and low CO₂ emissions, as demonstrated in a fluidized bed reactor-regenerator pilot plant. Studying the same catalyst, SAPO-34, Yang et al. [92] focused on enhancing the structural stability of the zeolite to improve its long-term durability after repeated regeneration cycles. They studied the effect of coke formation and water exposure on the zeolite structure. They observed that, after prolonged

exposure to moisture or continuous regeneration cycles, an irreversible hydrolysis of Si-O-Al bonds occurs, leading to framework degradation. To mitigate this, they explored several strategies, including water co-feeding, which extends the catalyst's lifetime before regeneration, although irreversible hydrolysis is still observed after 20 cycles. Another approach is catalyst pre-coking, which, when combined with water co-feeding, stabilizes the framework, ultimately enhancing catalytic efficiency and long-term stability. Recently, Zou et al. [93] attempted to improve the stability of a modified ZSM-5 zeolite by incorporating gallium to prevent rapid deactivation and reduce the frequency of catalyst regeneration. By adding liquid Ga, they successfully decreased coke deposition and enhanced the desorption of carbonaceous species. They demonstrated that stability is improved because the liquid Ga is located in the intercrystallite region and partially penetrates the micropores of ZSM-5, modifying the acidic properties of the zeolite to prevent deactivation. Furthermore, they concluded that co-feeding hydrogen enhances stability by a factor of 14 compared to conventional ZSM-5. Recent studies have shown that controlled steaming of SAPO-34 can redistribute framework Si and reduce acid site density, which, despite partial acid site loss, enhances catalyst lifetime in MTO by mitigating deactivation while maintaining olefin selectivity [94]. Similarly, hydrothermal treatment of ZSM-5 and its extrudates allows fine-tuning of Brønsted/Lewis acidity, leading to improved propylene selectivity and extended catalyst lifetime in the methanol-to-propylene process and they calin the final fuel properties have high similarity to that of jet fuel [95].

Another key approach in catalyst optimization focuses on improving selectivity towards desired products while minimizing the formation of unwanted byproducts. In this regard, the modification of ZSM-5 with Ga has been studied to modify the acidity of the zeolite and optimize both propylene selectivity (up to 45.3 %) and propylene/ethylene ratio (14.6) [96]. It was concluded that Brønsted/Lewis (B/L) ratio determines the lifetime of the zeolite, while the weak/strong acid site ratio governs the propylene/ethylene ratio. By incorporating Ga into zeolite framework (with an optimal Ga content of 1.3 wt%), it is possible to modify the acidity of the zeolite and optimize the coordination structure of Ga, achieving optimal results in selectivity and propylene/ethylene ratio, while enhancing the stability of the catalyst (> 180 h). Similarly, SAT-type molecular sieves have been studied to optimize the propylene/ethylene ratio [97]. By regulating the cage size and the density of acid sites, they successfully enhanced this ratio. Additionally, they analyze the composition and concentration of different hydrocarbon pool species produced at the beginning of the reaction by the studied catalyst to better understand the observed differences in the activity. Finally, they optimize the reaction conditions by varying temperature and WHSV, achieving an optimal ratio of propylene/ethylene of 4.17

4.5. Syngas-to- Ethanol (-to-Jet)

A promising and already ASTM-approved pathway for SAF production involves the conversion of syngas into ethanol, followed by its dehydration and subsequent oligomerization (ATJ-SPK pathway) to generate higher hydrocarbons suitable for jet fuel applications (see Table 5).

Ethanol production from syngas is limited by low conversion and

selectivity which also triggered extensive research on catalyst design [120]. Ethanol synthesis requires dual-function catalysts: one enabling CO dissociation (chain growth) and another for non-dissociative CO adsorption (alcohol formation) [121]. Achieving ethanol selectivity over other alcohols remains a major challenge [102,120]. An indirect tandem route using methanol was proposed by Kang et al. [102]. Their system combined ZnO-ZrO₂ (for methanol), H-MOR zeolite (acetic acid), and Sn-Pt/SiC (hydrogenation), achieving 9.7 % CO conversion and 64 % ethanol selectivity without intermediate separation.

Rhodium-based catalysts dissociate CO efficiently but favor CH₄. Adding Fe or Mn modifies selectivity toward ethanol. For instance, Rh-Fe/TiO₂ achieved 37 % selectivity [103–107], while Mn-Rh systems reached 27.3 % ethanol selectivity at 42.4 % CO conversion [108]. A RhMnFe/SiO₂ system combined benefits of both promoters, enhancing stability and selectivity [122–125]. Cu-based systems, though better for methanol, showed 24.9 % ethanol selectivity when promoted by Cs [126].

Non-noble metal catalysts offer industrial promise due to cost. MoS_2 , especially when promoted (e.g., with K_2CO_3 or Ni), achieved 20–42 % selectivity [109,110]. Among Mo compounds, activity decreases in the order: $MoS_2 > Mo_2C > MoOx > MoP$ [127].

Co-based catalysts traditionally used in FTS have been adapted for ethanol via tuning of CO adsorption properties. A Co-Ga-La-Sr perovskite yielded > 30 % ethanol selectivity [111], while Ni addition enabled dual CO adsorption modes, reaching 19.4 % ethanol selectivity [112]. Co-Cu-Mn systems reached 45.4 % ethanol among total alcohols, with Mn enhancing site activation [113].

After ethanol production from syngas, it needs to be dehydrated to be able to oligomerize and therefore produce SAF. Ethanol is industrially dehydrated using Al₂O₃ or HZSM-5, with ethylene yield improving above 250 °C [128]. Current research efforts are focused on catalysts that exhibit stability and perform effectively under mild operating conditions. in general, ethanol dehydration selectivity is relatively high (>70 %- Table 5) and process is well developed (part of AtJ) however acetaldehyde, diethyl ether and crotonaldehyde as major side products can form during ethanol dehydration through a bimolecular reactions [116]

 $Al_2O_3\text{-}carbon$ catalysts modified with ammonia showed 98.3 % conversion and 97 % selectivity due to added Brønsted acidity [114]. Mn/SiO2 systems improved with ZrO2 and Ni, linking acidity to performance [116]. Modified HZSM-5 (e.g., Ce-doping, lower Si/Al ratio) achieved 67 % selectivity to ethylene and 140 h stability [115].

SBA-15 silica modified with palm oil clinker or tungsten improved porosity and acidity, attaining 98.7 % selectivity at 400 °C [118,119]. Modified H-ZSM-5 via dealumination or OH treatment enabled full conversion at 220–225 °C with > 85 % selectivity [129,130]. Rho-type zeolites offered > 99 % selectivity across 250–400 °C [131].

Aquivion® PFSA, a perfluorosulfonic resin, showed high performance at 200 $^{\circ}$ C, especially when combined with TiO₂ to enhance porosity and mass transfer, raising productivity to 0.36 gethanol·min⁻¹·g-cat⁻¹ [117].

Lastly, mesoporous aluminosilicates offered stable, coke-resistant operation with moderate acidity and no textural loss, proving effective under mild conditions [132].

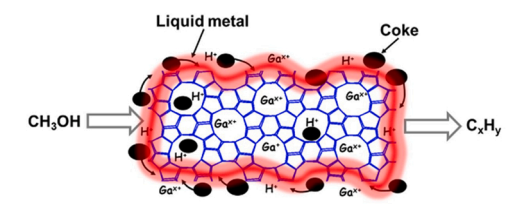


Fig. 3. Scheme of the effect of liquid metal on the MTH reaction by desorption of carbon species, reproduced with copywrite permission from ref. [93].

4.6. Olefin Oligomerization and Hydrogenation

Following olefin synthesis (either from MTO or direct FTO), oligomerization and hydrogenation are required to produce jet-range saturated hydrocarbons. Overall, the STO route with downstream oligomerization and hydrogenation offers modularity and flexibility in SAF production. However, integration, catalyst stability, and economic viability still require optimization to make this route competitive with direct STJ or FTS-based methods. According to a report from Pacific Northwest National Laboratory [70], oligomerization remains the key bottleneck at relatively low TRL for the MtJ approach, whereas upstream steps such as syngas-to-methanol, MTO, and hydrogenation are already demonstrated at TRL 9.

From a catalytic perspective, oligomerization of light olefins (C_2 – C_3) proceeds differently from that of higher olefins (C_4 *). Acidic solids such as zeolites (e.g., H-ZSM-5), sulfated oxides, and ion-exchange resins are effective for oligomerizing C_4 * olefins via carbocation mechanisms, while nickel-based catalysts are typically required for light olefins. Ni²* supported on mesoporous oxides (e.g., SBA-15, Al₂O₃) enables ethylene oligomerization through metallacyclic chain growth [133,134] though related Cossee–Arlman-type pathways have also been proposed [128, 130]. Metal–acid bifunctional systems (e.g., NiSO₄/Al₂O₃–Fe₃O₄, Ni–WO₃/Al₂O₃) can further tune performance, selectively favoring dimerization or trimerization depending on conditions [133,135]. Extra selectivity to certain HC length could be extra beneficial when for blending. A summary of catalysts for olefin oligomerization and hydrogenation toward SAF is given in Table 6.

De Klerk and co-workers demonstrated that even dilute FT tail gas (~7 % olefins) can be oligomerized over MFI-type zeolites to yield jetrange products, and that CO in the feed does not inhibit activity [136]. In contrast, oxygenates were shown to accelerate catalyst deactivation [137], with pretreatment improving stability. They further observed that co-feeding small amounts of water can mitigate coking, though excessive water reduces activity reversibly.

Ethylene (and partly propylene) oligomerization is particularly challenging because carbocationic pathways are inaccessible; instead, it requires transition-metal centers (e.g., Ni) to proceed via metallacyclic mechanisms at $<250\,^{\circ}\text{C}$ [135]. Although ethylene dimerization is thermodynamically favorable, the high activation energy and selectivity issues limit its utility in SAF contexts [138]. By contrast, higher olefins (C4*) oligomerize efficiently on acidic solids, making them preferred feedstocks for synthetic jet fuel production.

Recently, the van Bokhoven group [138] reported that the optimal feedstock for jet fuel production comprises C4 and C5 olefins. By carefully adjusting the ratios olefin of C3, C6, and C7 olefins, they demonstrated that product composition and fuel properties can be tuned effectively while in their earlier work [139], they observe that high reactivity of lighter olefins can suppress the reactivity of heavier olefins (this is also observed by others e.g. high reactivity of propene[140, 141]), altering branching and product range and that changing reaction parameter cannot effectively tune product composition and feed composition is main parameter when performing co oligomerization. Their experimental kinetic modeling further highlighted that excluding lower olefins like ethylene not only simplifies the process but also avoids excessive isomerization in the final product, a feature undesirable in jet fuel. This insight suggests that olefin streams derived from FTO may be more suitable for jet fuel synthesis than those obtained from MTO processes, which mainly yield light olefins. We believe this direction holds greater potential for efficient and selective jet fuel production though oxygenate adverse effect on oligomerization catalysts needs to be considered [137].

In summary, higher olefins (C_{+}^{+}) remain the most suitable feedstocks for oligomerization toward SAF. Light olefins, although mainly produced by MTO and ATJ-derived intermediates, present mechanistic and selectivity challenges that lower process efficiency. Future advances needed on tailored catalysts and feed conditioning strategies that can



Fig. 4. Tandem catalyst for the indirect production of ethanol via methanol, reproduced with copywrite permission from ref. [102].

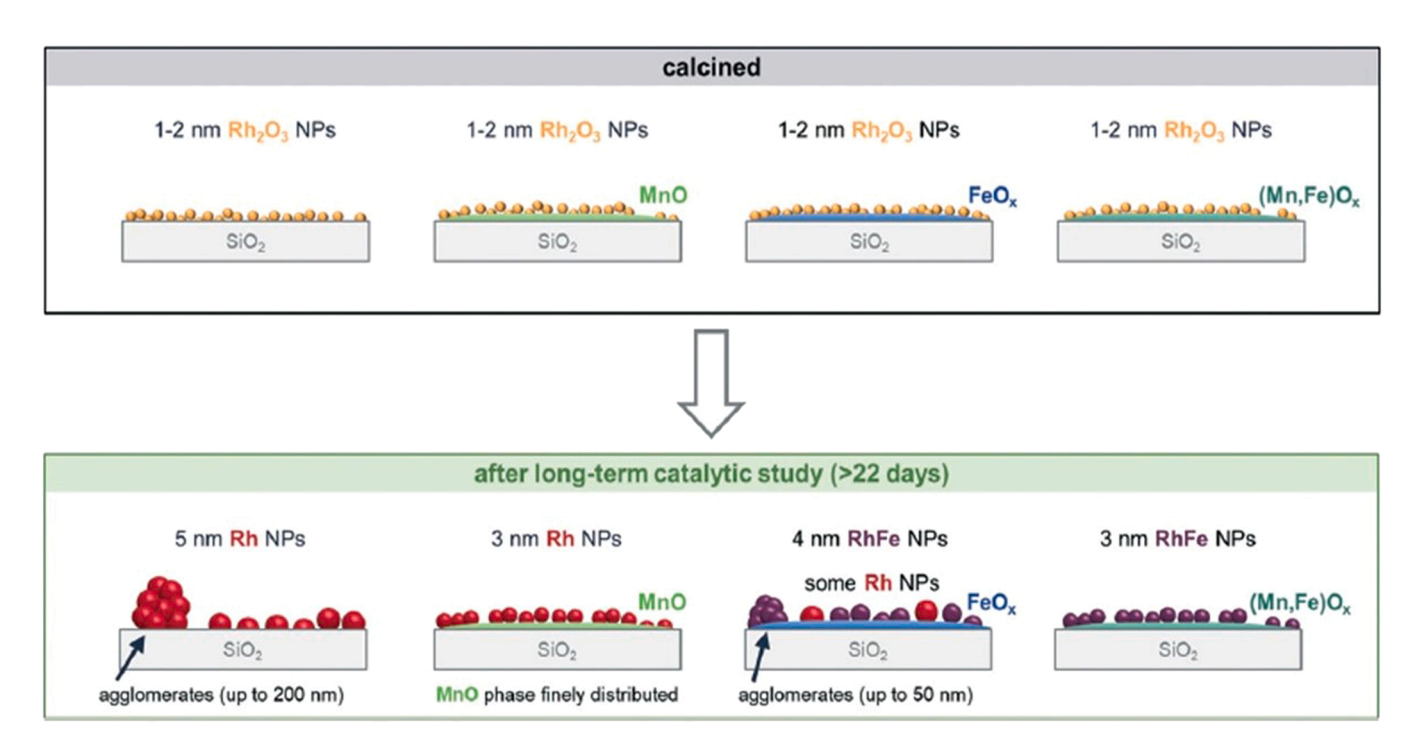


Fig. 5. Structural models after calcination and after long-term catalytic study, reproduced with copywrite permission [122].

overcome oxygenate sensitivity, suppress undesired isomerization, and maximize conversion to the desired C_8 – C_{16} jet fraction we further discuss the development in the area of light olefin oligomerization.

4.6.1. Light olefin oligomerization

Light olefin oligomerization (especially for ethylene) using homogeneous catalysts, such as nickel-phosphine complexes, is a wellestablished and industrially mature process, offering higher control over product selectivity and operating at relatively mild conditions compared to heterogeneous systems. Notable industrial examples include the Shell Higher Olefin Process [149] and Honeywell UOP's licenses [150,151], which use multi-step oligomerization and hydrogenation to convert ethylene into linear α -olefins and subsequently into fuels and lubricants. However, in the context of SAF production, which often relies on mixed-olefin syngas derived from biomass or waste gasification, heterogeneous catalysts are generally preferred not only for sustainability of process but also because branched/isomerized HCs are needed in jet fuels. These catalysts offer greater robustness, ease of separation, and adaptability to mixed-feed conditions. Ethylene conversion over acidic heterogeneous catalysts (e.g., zeolites or aluminosilicates) typically require temperatures exceeding 300 °C due to their inability to form stable carbenium intermediates, which are crucial in acid-catalyzed pathways. In contrast, C₃+ olefins, such as propylene and butenes, can undergo oligomerization at lower temperatures (100–250 $^{\circ}$ C) via carbocationic mechanisms facilitated by Brønsted acid sites. In nickel-catalyzed ethylene oligomerization, butenes are typically the dominant products, which can then undergo further oligomerization more readily than ethylene itself. The challenge with ethylene lies in its inability to stabilize a carbenium ion, thus limiting its reactivity in acid-driven mechanism. The inability to form the carbenium transition state for ethylene inhibits the carbenium mechanism. For optimal results, olefin oligomerization should be conducted at lower temperatures to produce longer-chain olefins, while avoiding side reactions such as aromatization, transfer hydrogenation and cracking [152]. Transition metal based catalysts enable the oligomerization of ethylene at temperatures below 200 °C [153] and if combined in bifunctional catalyst with acid sites can be used to produce fuels. Generally, achieving high yields of jet fuel range products relies significantly on the use of highly selective catalysts with well-defined pore size and metal and acid sites ratios and this can be done either on one catalyst having dual functionality or having metal catalyst and acid catalyst acting separately which will be further explained in the next subsections.

4.6.1.1. Two-stage oligomerization or cascade oligomerization. Generally, the oligomerization in one step is not enough to obtain jet fuels with high selectivity on a single catalyst (either metal based or acid based [142]). With the aim of enhancing the production of jet fuel range oligomers, Babu et al. proposed an integrated two-stage process for oligomerization of ethylene and light olefins. In the first stage, Ni-AlSBA-15 catalyst exhibited high catalytic activity, yielding over

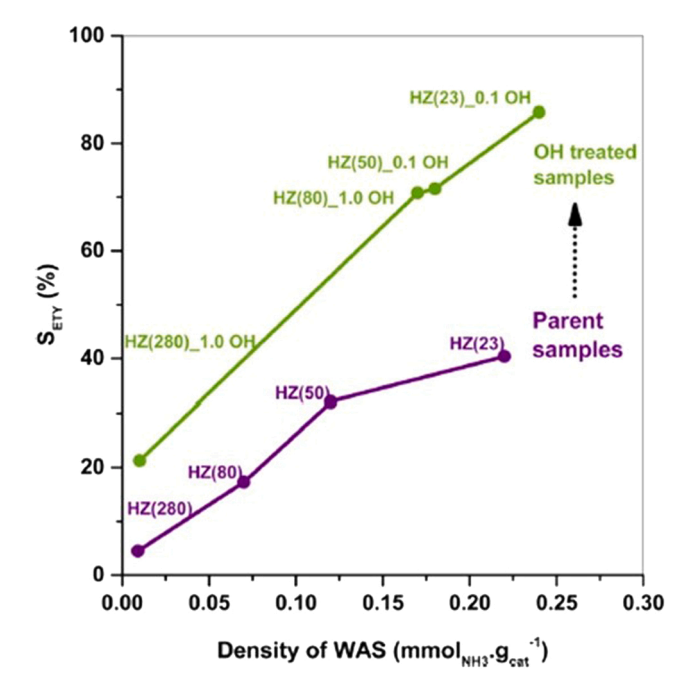


Fig. 6. Correlation between ethylene selectivity (at similar ethanol conversion) and the density of weak acid sites for parent (purple) and OH-treated (green) HZSM-5, reproduced with copywrite permission from ref.[129].

99 % ethylene conversion with non-ASF type distribution of the generated HCs ($C_8 > C_6 > C_4 > C_{10}$) and high stability at 200 °C and 10 bar. Subsequently, the liquid mixture obtained in the first step underwent co-oligomerization using Amberlyst-35 ion-exchange resin. Operating conditions of 100 °C and 30 bar of N₂ yielded a liquid product ($C_{10} > C_8 > C_6 > C_4$) compromising over 98 % C_{5+} , with C_{10+} olefins accounting for approximately 42 % [147]. Others also tried to apply similar strategy to improve the selectivity of light olefins oligomerization to SAF [72]. A similar strategy to optimize selectivity towards jet-range products involves employing two catalysts in the series within the same reactor [70, 142]. Compared to the catalytic results from reactions with the single catalysts under identical conditions, the one-pot cascade Ni/Siral-30 and HZSM-5 studied by Kwon et al. [142] exhibited close to 100 % conversion and resulted in a completely reversed Schulz-Flory type distribution ($C_{10+} > C_8 > C_6 > C_4$), and yielded the highest amount of liquid

product for the entire reaction time at 250 °C. First, each catalyst was tested independently at different reaction temperatures. The results obtained are depicted in Fig. 8. H-ZSM-5 was not reactive at temperature below 250 °C. Above 300 °C, the selectivity of C₁₀₊ products was higher than Ni/Siral-30, but the ratio of non-cyclic linear HCs to aromatics was 10/90, contributing to a significant production of aromatics. On the contrary, Ni/Siral-30 exhibited a high conversion at low temperatures, but the selectivity of C₁₀₊ was low. Thus, the combination of both catalysts could lead to jet-fuel range HCs production, while avoiding the formation of excessive aromatic products. At 250 °C, high ethylene conversion, selectivity to C₁₀₊, and liquid yield was achieved, compared to 200 and 300 $^{\circ}$ C. Moreover, the H-ZSM-5 was treated with NaOH (HZSM-5–5B) to study the modification of the catalyst properties. It was confirmed that NaOH treatment of H-ZSM-5 can alter the product distribution, specifically shifting the ratios of C₁₀₋₁₉ to C₂₀⁺ hydrocarbons and adjusting the balance between linear non-cyclic hydrocarbons and aromatics [142]. In general, extra advantage of zeolite active in aromatization of olefin (e.g. ZSM-5) is that they can also produce aromatics which are needed in current jet fuel formulation (Table S1) and they can also be hydrogenated to include cycloalkanes.

In line with this strategy, Mohamed et al. [148] proposed a dual-bed system. Initially, ethylene dimerization was performed using a Ni catalyst supported on H-Y zeolite, followed by oligomerization over a H-ZSM-5 zeolite. As depicted in Fig. 9, the Ni/Y catalyst produces C4 olefins, while the H-ZSM-5 zeolite is essential for producing jet-fuel range products. Selectivity and deactivation of the catalyst were studied as a function of catalyst acidity, temperature, and bed configuration. It was concluded that zeolites with higher acidity (lower Si/Al) enhanced catalytic activity. Regarding catalyst deactivation, the dual-bed method demonstrated efficiency in preserving the oligomerization catalyst (H-ZSM-5) from deactivation due to coke deposition compared to the initial Ni/Y dimerization catalyst, which deactivates at a faster rate. Nevertheless, the catalysts are unable to maintain the activity over extended periods. With the optimized conditions, the dual-bed setup achieved a jet fuel range product selectivity exceeding 50 % for over 20 h. However, the ethylene conversion decreased significantly during the reaction [148].

4.6.1.2. One-pot direct oligomerization. While we mentioned that, in general, one step oligomerization is not sufficient to obtain high SAF selectivity, a few groups [143,144] have shown that by preparing a complex pore structure and achieving a high residence time of intermediate olefins, it is possible to obtain relatively high selectivity to

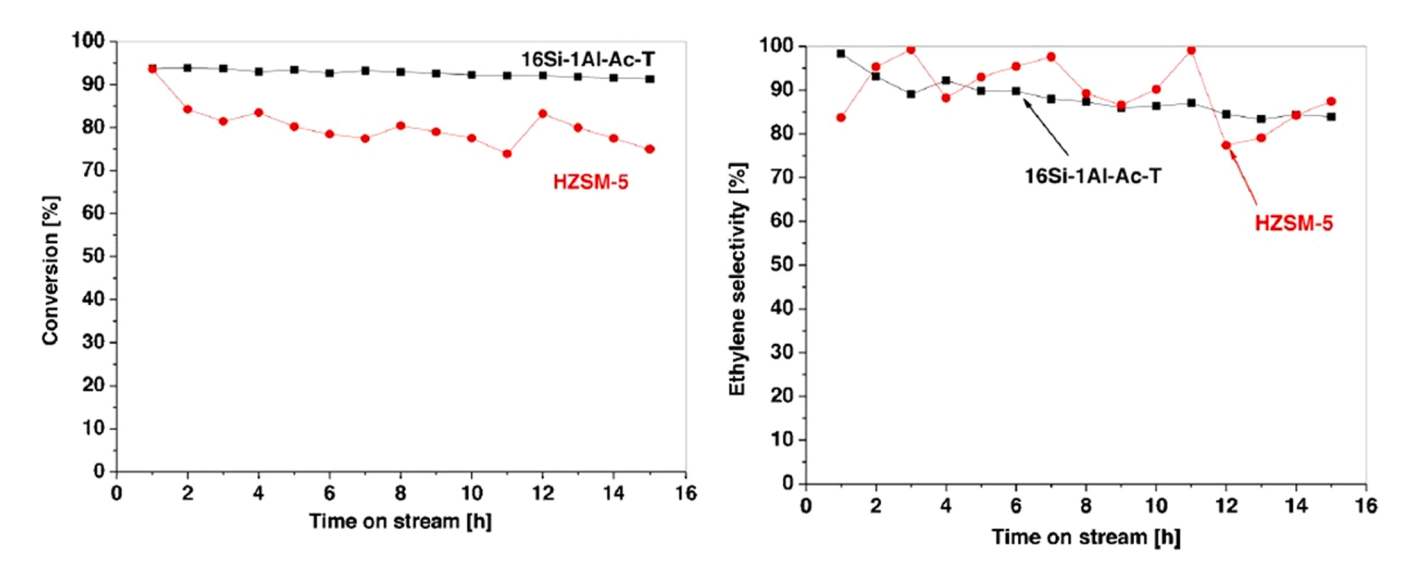


Fig. 7. Conversion (left) and ethylene selectivity (right) over HZSM-5 and 16Si-Al-Ac-T at their maximum productivity, reproduced with copywrite permission from ref. [132].

Table 5 summary of catalyst for syngas to ethanol and other higher alcohol conversion as well as catalyst for their dehydration and oligomerization.

Step	Catalyst System	Function / Notes	performance	T (°C)	P (bar)	H ₂ /CO or M	TOS (h)	By-products / CO ₂ selectivity
Syngas → EtOH / higher alcohols	Rh/Fe [103–107], Rh/Mn [108]	Tuned for CO insertion and C_2+ alcohols; interfacial effects	C= 42.4 % EtOH= 27.3 % (Mn-Rh); Rh-Fe/TiO ₂ up to 37 % EtOH	290	30	2	n.r.	Rh tends to CH ₄ ; promoters shift to ethanol.
	MoS ₂ + K [109], Mo-Ni-K[110]	Non-noble option; suppresses methane	C= 20 %, S= 20 % C= 41 %,S= 42 %	280–330 330	90 10	1 1	n.r.	Activity order noted: MoS ₂ > Mo ₂ C > MoO ₃
	La, Sr, Co and Ga perovskite	Perovskite precursor → tailored Co	C= 4–10.5 %, ~ EtOH S= 30 %	310	40	0.5–3 Optimal= 2	200	> MoP. CO ₂ = 3–10 %, other alcohols C1 and C3 $+$
	Ni / Co-Co ₂ C catalyst [112]	Dual CO adsorption modes	EtOH= 19.4 % (45.2 % in liquids) C= 12.8 %	260	30	2	n.r.	$CO_2 = 1.6$ $GHSV = 6600 \ h^{-1}$
	Co-Cu, Co-Cu-Mn[113]	$Cu \rightarrow MeOH sites; Co \rightarrow chain growth$	46.2 % total ROH (45.4 % EtOH in ROH) CO C= 29.7 %	270	25	2	96	Mn enhances site activation. GHSV = 7500 h^{-1} ,
	Indirect tandem (Kang et al. [102])): (1) syngas→MeOH K-ZnO-ZrO₂; (2) MeOH→AcOH H-MOR; (3) AcOH→EtOH Sn-Pt/SiC	Indirect route without intermediate separation	C= 9.7 %; S= 64 %	310	50	1	100	Three-step tandem system.
Alcohol (EtOH)→ Ethylene (dehydration)	NH ₃ -modified γ-Al ₂ O ₃ on carbon [114]	Traditional dehydration; added Brønsted acidity	C= 98.3 %, S= 97 % Y= 95.4 % (for plain γ-Al ₂ O ₃ S=45 %)	450	1	_	150	WHSV = 4.73 h^{-1} , C reduced to 70 % after 150 but then stable
(,,	HZSM-5 (Si/Al; Ce/Cu-doped) [115]	Lower-T dehydration improved stability	C= 100 % S= 67 %;	300	1	_	140	WHSV= $42.3 h^{-1}$
	Mn-Ni/SiO ₂ -ZrO ₂ [116]	Tuned acidity for selective ethylene	C> 98 % S: 77 % Y= 75 %	350.	1	_	800	WHSV= $1.4 h^{-1}$
	Aquivion® PFSA + TiO ₂ [117]	Mild-T dehydration, high activity	S and C > 90 % at 200 °C	120–200	1	_	14	WHSV 0.025–0.15 h ⁻¹ Diluted EtOH stream 1 %
	SBA-15 (derived from POC and water feeding) [118] W-SBA-15 and W-MCF-Si [119]	Mesoporousacid- tunable; long-term	S= 84.7 % C > 73 % S= 98.7 %, C> 99 %	400 400	1	_	150 10	EtOH stream 50 % LHSV = 16 mL/g·h Water co-feeding improves S EtOH Conc.= 70 %

^{*}Palm oil clinker waste (POC), C:Conversion, S:Selectivity, Y:Yield=C*S, GHSV: gas hourly space velocity, LHSV=liquid hourly space velocity, weight hourly space velocity: WHSV.

SAF-range HCs on a single catalyst. Several nickel-based catalysts supported on microporous aluminosilicates have been studied for ethylene oligomerization. Moon et al. conducted ethylene oligomerization using NiH- and H- forms of ZSM-5 and beta zeolite catalysts. The Si/Al and Ni content were maintained constant to study the differences in the textural properties. Crystal size and mesoporoity of the catalysts were varied through sophisticated constructive and destructive techniques. The combination of nanocrystallinity and intercrystalline mesoporosity obtained in the catalyst resulted not only in high initial activity and stability but also high selectivity towards jet fuel range products. The oligomerization of ethylene under 35 bar and 200 °C over the optimized catalyst exhibited remarkable C₁₀₊ product selectivity higher than 80 % [144]. With the aim of simplifying the catalyst synthesis, Ni was impregnated on a commercial SIRAL-30 support with a high Brønsted acid site density (Fig. 10). The support exhibited a high Si/Al ratio, resulting in high surface acidity, which enhanced the activity of the catalyst. Moreover, optimal conversion and selectivity to C₁₀₊ were achieved with a 4 % Ni loading. Finally, pretreatment under N2 atmosphere at 550 °C proved advantageous for enhancing both the dispersion of Ni²⁺ species and Brønsted acid site density. Despite achieving relatively low selectivity (approximately 20 %), the stability of this catalyst makes it a noteworthy system. Moreover, while some deactivation was observed in the used catalyst due to the adsorption of heavy oligomers, the initial catalytic activity was effectively restored by treating the catalyst at 550 °C in an air atmosphere. The catalytic results for fresh and regenerated catalysts are summarized in Fig. 10 [143].

Being aware of the importance of Ni impregnation step, different catalysts were synthetized by both one-pot synthesis employing Niligands and post-synthesis approach. The former method promoted the formation of NiO nanoclusters within the zeolitic pores. Conversely, the post-synthesis impregnation resulted in a higher content of Ni^{2+} in ion exchange position, with the stabilization of these species being favored for zeolites with higher Al content. It was demonstrated that the post-synthesis approach exhibited higher activity. However, higher selectivity to jet fuel range products was obtained when the catalyst was synthesized by one-pot employing Ni-ligands. Additionally, it was concluded that crystallite size plays a crucial role, with nano-sized zeolites proving to be more active and stable towards deactivation. Therefore, the methodical synthesis of Ni-containing zeolites, controlling both the zeolite topology and crystal size, as well as the Ni speciation and acidic properties of the support, enables the enhancement of both initial activity and catalyst life. The achieved maximum yield rose to 45 % at 200 °C and 35 bar [154].

Furthermore, mesoporous silica modified with aluminum has been investigated as support. Subsequently, Ni was impregnated to alter the physicochemical properties. Ni-AlSBA-15 appeared as a promising catalyst for the oligomerization to produce bio-jet fuel range HCs. The selectivity towards C_{10+} products was enhanced at higher temperatures, higher pressures and lower weight hourly space velocity (WHSV). Moreover, the catalyst demonstrated prolonged stability throughout long-term catalytic test [155]. Similarly, mesoporous Ni-AlKIT-6 was synthetized through wetness impregnation method to load Ni. The effect of the Si/Al ratio was investigated, concluding that higher Si/Al ratio enhanced the ethylene conversion. The acidity of the catalyst varied according to the amount of Al incorporated in the silica framework, with higher Al content resulting in lower acid strength. Moreover, high Al

Table 6Summary of catalyst for oligomerization and hydrogenation.

Method	Catalyst System	Function	Reported performance	T (°C)	P (bar)	TOS (h)	Extra note
Direct (1 cat)	amorphous silica-alumina (ASA) [137]	FT tail gas; aimed for distillates (not SAF)	Conv. > 80 % (purified feed w/o oxygenates)	110–300	6	70 days (pilot scale)	-
	4 %Ni/SIRAL-30 [142,143]	One-pot oligomerization	Conv. $> 99 \%$, $\approx 40 \% C_{8}$ – C_{16}	200	10	100	$C_{10}^* = 15-20 \%$
	5 %Ni/SIRALOX 40 [74]	Co-oligomerization	Selectivity > 90 %, C ₈ –C ₁₆	120	32 (Pt	24	S> 90 % iso
	1.9 %Ni/SIRALOX 40 [141]	$(C_2^=-C_4^=)$; reg. at 300 °C Feed= $C_2^=$	main fraction C: $C_2^= > 99 \%$	120	= 40) 50	170	High iso. in heavier HC ${ m C_5~C_{12}}$ WHSV= ${ m 8~h^{-1}}$
	NiH-ZSM5 NiH-Beta [144] (nonosheets and nano sponges)	One-pot; mesoporosity improves conversion	C ₂ H ₄ conv. 20–80 %; > 80 % C ₈ –C ₁₆ (higher selectivity ZSM–5; higher conversion BEA)	200	35	900	C ₁₀ * > 80 %; WHSV 2.5 h ⁻¹
	Ni-AlKIT-6 (varying Si/Al) [145]	C ₂ oligomerization; acidity controls selectivity	$C>95~\%;$ $C_8^{\star}\approx55~\%$	300	20	6	$WHSV = 0.6 \ h^{\text{-}1}$
	NiSO ₄ /Aluminosilicate[146]	C ₂ –C ₄ feed	Conv. $> 70 \%$; C ₈ –C ₁₆ $> 75 \%$	280	40	12	Iso/n> 90 % , % arom.=9 %
2 step or sequential catalytic system	Ni/Al-SBA-15 [147] Firt part (second part) Amberlyst-35 [147]	Two-step (acidic + resin)	99 % C_2H_4 conv.; ≈ 7075 % $$C_8C_{16}$$	200 / 100	10 / 30	60	$C_8 > C_6 > C_4; \ C_{10}{}^* = 42 \ \%$
•	H-ZSM-5/ Ni/SIRAL-30 [142]	Reverse Schulz–Flory distribution	Conv. $> 90 \%$; $\approx 55 \% C_8$ – C_{16}	250 (opt.)	10	16	30 % aromatics; C ₁₀ * = 36 %
	2 %Ni/SIRALOX / SIRALOX 40 [73]	Co-oligomerization (C_2-C_4)	$\approx 85~\%$ $C_{\text{8}C_{16}}$	120	32 (pt = 40)	216	C ₃ –C ₄ decreased after 100 h; C ₂ stable
	Ni/Y- ZSM-5[148]	Dual-bed cascade	Conv. > 50 %; 64 wt% C ₈ –C ₁₆	300	35	20	_
	Metal followed by acid catalyst (exact composition is not reported) [70]	sequential catalyst feed: equimolar C2-C3	Conv. ~ 90 %; ~70 % C ₈ -C ₁₆	275	6.9	22	Mix system deactivate Fastly but sequential loading were stable WHSV: 0.8 h ⁻¹
	State-of-the-art nickel catalysts followed by acidic resin [72]	sequential catalyst C ₂ -C ₃	n.r.	n.r.	n.r.	n.r.	n.r.
H*	Pd/H-ZSM-5 [87] As example Hydrogenation metals/zeolite Ni-W-S	Post-oligomerization hydrogenation	Example case; fully saturated paraffins	100–250	20–40	n.r.	WHSV 0.5-4 h ⁻¹
	Ni, Pd, Pt / Al ₂ O ₃ or C [77]	Generic hydrogenation	C> 99 %	50-370	5-50	n.r.	_

^{*} H=Hydrogenation, C:Conversion, S:Selectivity, Y:Yield=C*S, weight hourly space velocity: WHSV, Pt= total pressure.

content changed the structure of KIT-6, decreasing the catalytic activity. On the other hand, high acid strength promoted aromatic HCs. Thus, the optimal Si/Al ratio was determined to be 5 [145].

4.7. ASTM certification status of discussed routes

The ASTM certification status in Table 7 clarifies the readiness of the syngas-derived pathways discussed in this review. Established routes such as FT-SPK (Annex A1) and ATJ-SPK from ethanol (Annex A5/A8) are already approved for up to 50 % blending with conventional jet fuel and can be deployed commercially within existing aviation fuel frameworks.

In contrast, other pathways remain outside of the current ASTM annexes. MtJ has been formally submitted for ASTM D7566 approval in 2023 and is under review. If approved, this annex is expected to allow up to 50 % blending and could also cover olefin-to-jet processes that share the same oligomerization and hydrotreating steps. This development would significantly shorten the certification pathway for STO routes based on C_2 – C_4 olefin intermediates as well.

For STO-based approaches, ASTM compliance is currently only achievable if the olefin intermediates originate from ethanol, thereby aligning with the ATJ-SPK annex. In this review, STO is split here into two main variants: the mixed oxide catalyst route and the FTO route. Both require oligomerization and hydrogenation to yield paraffinic jetrange HCs suitable for ASTM consideration. However, FTO produces longer HCs, which means less oligomerization is required, and the resulting product contains a larger share of linear molecules, while the mixed oxide–zeolite system is more similar to MtJ once fully developed.

An additional advantage of routes involving olefins as intermediates is their versatility, as olefins can be further converted into a wide range of chemicals and materials, such as surfactants, aromatics, lubricants, and plastics, enabling broader utilization of sustainable feedstocks and meeting future demand for renewable chemicals. The olefin can also be used to produce cycloalkanes and aromatics needed in future jet fuels.

Direct syngas-to-jet pathways via integrated catalytic systems (e.g., bifunctional FTS + upgrading) are also not yet certified and would require the creation of a new annex before commercial adoption. In this context, it is worth noting that Klerk et al. [9] has proposed FT-based strategies that incorporate additional aromatic production steps, enabling the creation of a fully synthetic jet fuel (FT-SPK/green A) that meets ASTM aromatic requirements without blending. Such strategies not only address the regulatory need for aromatics but also increase the overall selectivity toward jet-range HCs, thereby improving process efficiency and commercial viability.it is also worth noting that aromatic presence cause also soot formation as mentioned earlier and in future once sealing issue is solved, aromatic free jet fuel will be desired however presence of cycloalkanes is always desired in jet fuel to improve density and cold flow properties.

Ultimately, the commercial adoption of novel syngas conversion routes will depend not only on catalytic performance and process economics but also on their ability to comply with ASTM D7566 standards, either through existing annexes, forthcoming approvals, or the establishment of entirely new certification pathways.

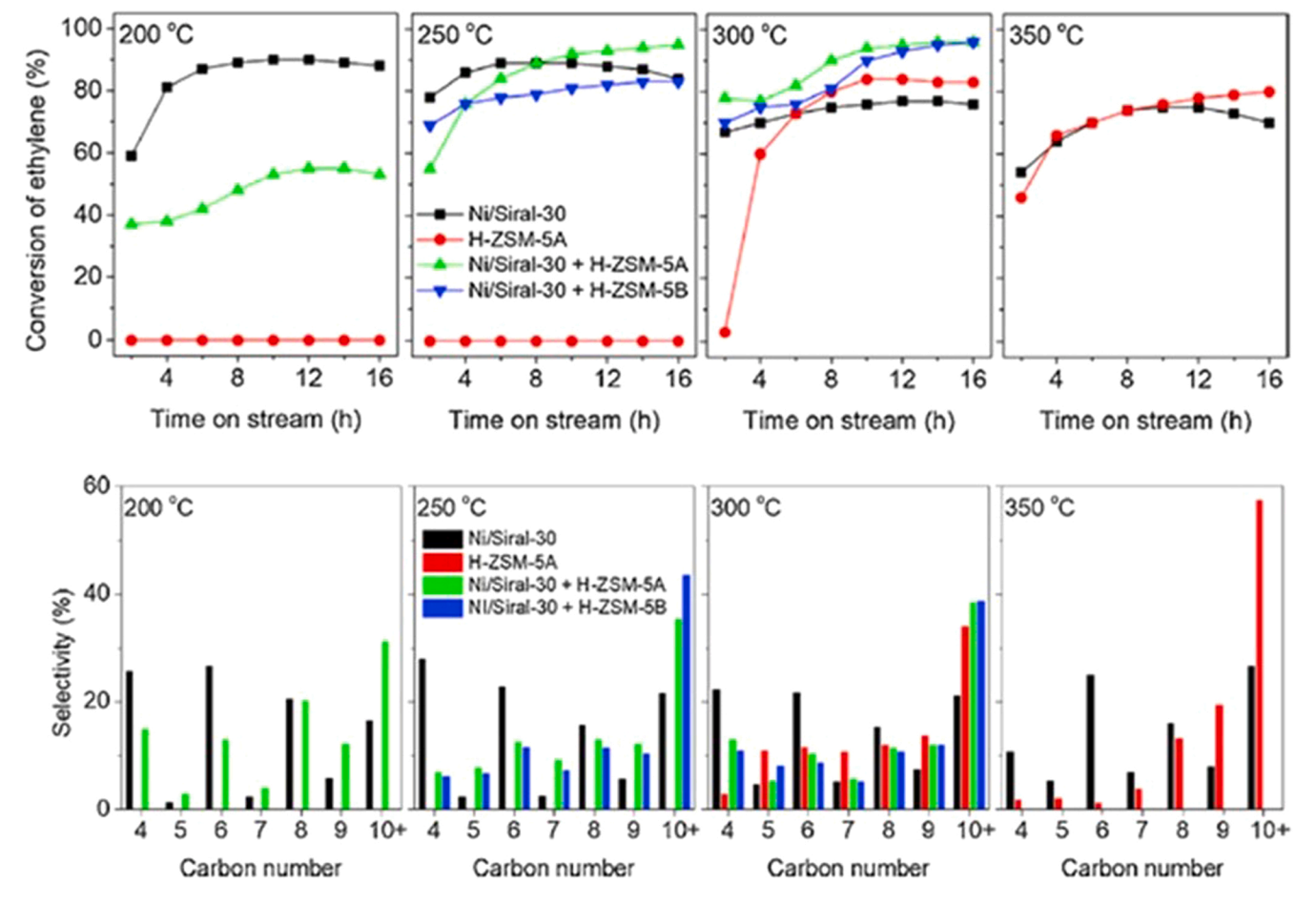


Fig. 8. Conversion (up) and carbon distribution after ethylene reaction for 16 h on stream (down) over different catalytic configurations, reproduced with copywrite permission from ref. [142].

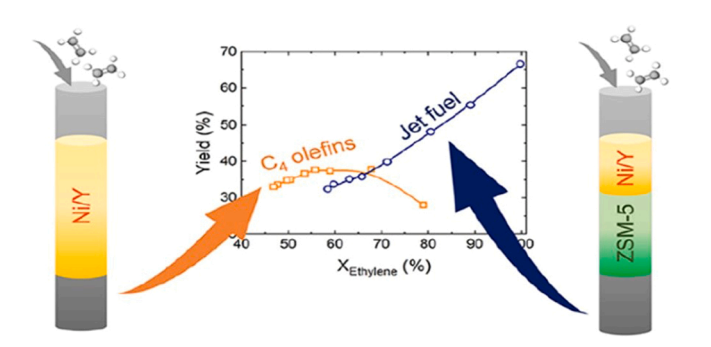


Fig. 9. Dual-bed strategy for enhancing jet-fuel range olefins, reproduced with copywrite permission from ref. [148].

5. Conclusion

As the aviation sector pushes toward carbon neutrality, syngas-based routes for producing SAF are emerging as flexible and future-proof alternatives. These technologies can tap into a wide range of feedstocks, from biomass and waste to CO_z and renewable hydrogen, making them especially attractive in a world that demands both sustainability and resilience.

Among the different options, FTS remains the most established and commercially deployed pathway. It's already ASTM-certified and supported by decades of industrial experience. Still, its broad product distribution limits how much jet fuel can be produced directly, which means additional upgrading steps are usually needed. Ongoing research

into more selective catalysts, like bifunctional and core–shell systems, is helping to push FTS closer to jet-fuel-specific designs, especially for smaller, decentralized plants.

To simplify the process and boost efficiency, STJ approaches aim to combine synthesis and upgrading in one step. With the help of advanced catalyst structures, these systems can bypass some of the limitations of traditional FTS. While still early in development, STJ holds great promise, particularly for compact and modular SAF production units.

The STO pathway, followed by oligomerization and hydrogenation, offers a more targeted approach to building jet-range HCs. By focusing on light olefins as intermediates, this route allows greater control over the carbon chain and product quality. Tandem catalysts and hybrid systems have made notable strides in improving both selectivity and efficiency, although their long-term stability and integration still require work.

Finally, alcohol-based routes, including MtJ and ethanol-to-jet processes, are gaining momentum. Methanol is already a well-established syngas product, and new MtJ platforms are showing good selectivity toward jet-range HCs. These routes are especially appealing when paired with renewable power and CO₂ capture. Ethanol-based strategies, while less mature, offer another interesting path, particularly with recent advances in catalyst design aimed at improving ethanol yield and selectivity.

In summary, there's no single "best" route to SAF from syngas, but rather a growing toolbox of catalytic options, each with strengths that suit different feedstocks, plant scales, and integration scenarios. Continued innovation in catalyst development, process integration, and fuel certification will be essential to move these technologies from promising lab results to real-world impact. With the right support,

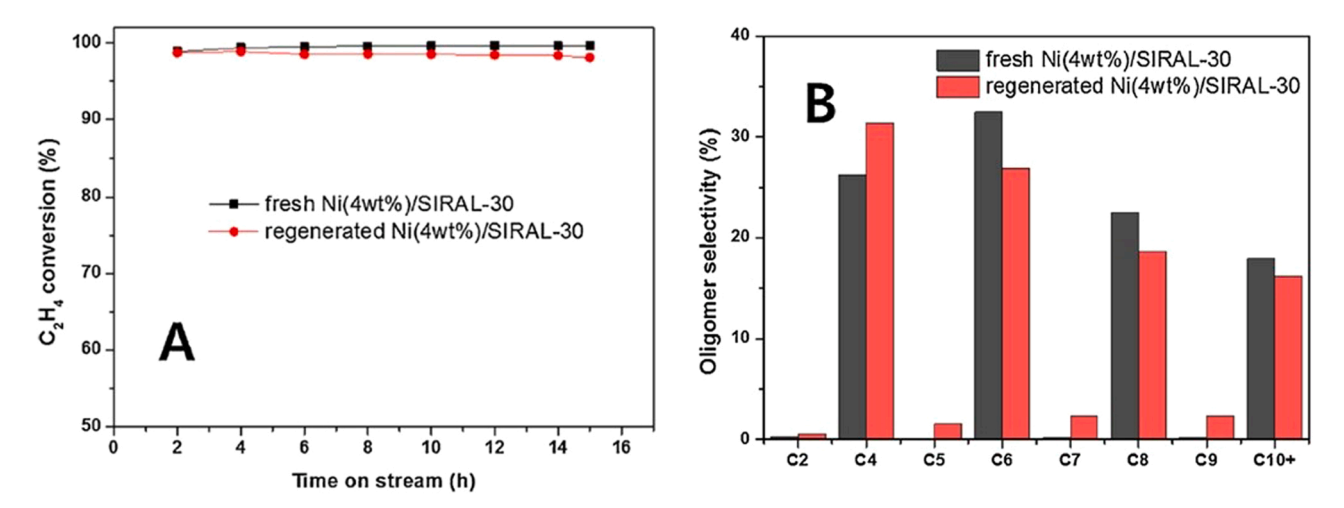


Fig. 10. Ethylene conversion and product selectivity over fresh and regenerated Ni/SIRAL-30. Reproduced with copywrite permission from ref. [143].

Table 7
Summary of syngas-to-jet fuel pathways discussed in this review, including ASTM certification status, technology readiness level (TRL), typical jet-range selectivity, and major technical challenges.

Pathway (discussed in this review)	ASTM D7566 Annex	Max certified blend (% vol.)	Status	TRL *	Typical jet- range selectivity (% C ₈ –C ₁₆)	Major technical challenges-extra advantages
FT-SPK	Annex A1	50	Certified	9	25–45	Requires separate hydrocracking/ isomerization; less selectivity, low in aromatics and high amount n-paraffin [156]
FT-SPK/green A with Aromatic from sustainable sources [9] [‡]	-	_	Not yet certified	5	> 60	Need at least 5 separate units for production: FTS, separation, oligomerization-alkylation, hydrotreating, aromatization, hydrocracking
STO – Mixed oxide catalyst route (direct syngas to olefins) + oligomerization + hydrogenation	-	-	Not certified (could be aligned with MtJ once it is certified)	4–6	60–75	RWG activity of mixed oxide catalyst $+$ high CO_2 selectivity (On the other hand, suitable for CO_2 and green H_2 stream), unknown long-term stability
STO – FTO (Fischer–Tropsch to olefins) + oligomerization + hydrogenation	-	-	Not certified (could be aligned with FT- SPK/A in new annex or MtJ if only light fraction of olefin is used)	4–6	55–85	Controlling olefin/paraffin ratio (especially in light fraction); post oligomerization may suffer from oxygenates [137]; CO ₂ management in Fe based cat. High price of Ru based one.
Alcohol-to-Jet via ethanol (ATJ-SPK)	Annex A5, Annex A8	50	Certified	7–8	60–80	hydrogen demand in hydrotreating, sometimes high branching of product [156], low yield of ethanol from syngas
Alcohol-to-Jet via methanol (MtJ)	ASTM submission under review (2023)	TBD (likely 50)	Pending certification	6	55–80	Need robust oligomerization catalyst, can include aromatics depending on oligomerization catalyst.
Direct syngas-to-jet via hybrid catalysis (e.g., FTS + upgrading in one reactor)	-	-	Not yet certified	3–4	45–60	Balancing FT and upgrading functions; unknown long-term stability of catalysts. Outperform FT alone as it can produce aromatic and isomers (least step required for jet fuels production)

^{*} TRL = Technology Readiness Level, based on literature, industry developments, and ongoing projects (e.g., Metafuels, Take-Off). Values are approximate and for indicative purposes, ‡-note that FT-SPK/green A is different than FT-SPK/A where aromatic is come form coal.

syngas conversion could play a central role in delivering the sustainable fuels that aviation needs for a cleaner future.

CRediT authorship contribution statement

Nerea Viar: Writing – review & editing, Writing – original draft, Visualization, Formal analysis. Berend Vreugdenhil: Writing – review & editing, Project administration, Funding acquisition. Iker Agirrezabal-Telleria: Writing – review & editing, Writing – original draft, Visualization, Formal analysis. Evert Boymans: Writing – review & editing, Writing – original draft, Visualization, Methodology, Formal analysis, Conceptualization. Yadolah Ganjkhanlou: Writing – review &

editing, Writing – original draft, Visualization, Supervision, Investigation, Formal analysis, Conceptualization.

Declaration of Competing Interest

The authors declare that they have no known competing financial interests or personal relationships that could have appeared to influence the work reported in this paper.

Acknowledgements

The authors acknowledge support from the ICARUS project, which

has received funding from the European Union's Horizon Europe research and innovation programme under Grant Agreement No. 101122303.

Appendix A. Supporting information

Supplementary data associated with this article can be found in the online version at doi:10.1016/j.apcata.2025.120554.

Data availability

Data will be made available on request.

References

- IATA. Sustainable Aviation Fuels. (https://www.iata.org/en/programs/sustainability/sustainable-aviation-fuels/), 2025 (accessed June 1, 2025).
- [2] B.H.H. Goh, C.T. Chong, H.C. Ong, T. Seljak, T. Katrašnik, V. Józsa, J.-H. Ng, B. Tian, S. Karmarkar, V. Ashokkumar, Recent advancements in catalytic conversion pathways for synthetic jet fuel produced from bioresources, Energy Convers. Manag 251 (2022) 114974, https://doi.org/10.1016/j.enconman.2021.114974.
- [3] K.S. Ng, D. Farooq, A. Yang, Global biorenewable development strategies for sustainable aviation fuel production, Renew. Sustain. Energy Rev. 150 (2021) 111502, https://doi.org/10.1016/j.rser.2021.111502.
- [4] FAME and HVO fact sheets. ETIP Bioenergy. (https://old.etipbioenergy.eu/fact-sheets), 2025 (accessed June 1, 2025).
- [5] Oils & Fats International (OFI). EU Biodiesel: Towards HVO. Oils & Fats International, (https://www.ofimagazine.com/content-images/news/Biofuels-HVO-takes-off-in-Europe.pdf), Issue February 2021 (accessed June 1, 2025).
- [6] Transport & Environment. European and US used cooking oil demand increasingly unsustainable. (https://www.transportenvironment.org/articles /european-and-us-used-cooking-oil-demand-increasingly-unsustainable-analysis), 2025 (accessed June 1, 2025).
- [7] Reuters. China pivots to Europe for used cooking oil exports as tariffs hit shipments to US. (https://www.reuters.com/sustainability/climate-energy/chin a-pivots-europe-used-cooking-oil-exports-tariffs-hit-shipments-us-2025-04-3 0) (accessed June 1, 2025).
- [8] Jasper Faber, David Lee, Bethan Owen, Potential for reducing aviation's non-CO₂ emissions through cleaner jet fuel. CE Delft, \(\hat\text{https://cedelft.eu/wp-content/uploads/sites/2/2022/03/CE_Delft_210410_Potential_reducing_aviation_non-CO2_emissions_cleaner_jet_fuel_FINAL.pdf), 2021 (accessed June 1, 2025).
- [9] A. de Klerk, G. Chauhan, C. Halmenschlager, F. Link, N. Montoya Sánchez, B. Gartley, H.E.M. El-Sayed, R. Sehdev, R. Lehoux, Sustainable aviation fuel: pathways to fully formulated synthetic jet fuel via Fischer–Tropsch synthesis, Energy Sci. Eng. 12.2 (2024) 394–409, https://doi.org/10.1002/ese3.1379.
- [10] Y. Ganjkhanlou, E. Boymans, B. Vreugdenhil, Minireview: intensified Low-Temperature Fischer-Tropsch reactors for sustainable fuel production (1-24), Fuels 6 (2025) 6020024, https://doi.org/10.3390/fuels6020024.
- [11] A. Delparish, A.K. Avci, Intensified catalytic reactors for Fischer-Tropsch synthesis and for reforming of renewable fuels to hydrogen and synthesis gas, Fuel Process. Technol. 151 (2016) 72–100, https://doi.org/10.1016/j. fuproc.2016.05.021.
- [12] Z. Gholami, Z. Tišler, V. Rubáš, Recent advances in Fischer-Tropsch synthesis using cobalt-based catalysts: a review on supports, promoters, and reactors, Catal. Rev. 63 (2021) 512–595, https://doi.org/10.1080/01614940.2020.1762367.
- [13] J. Li, G. Yang, Y. Yoneyama, T. Vitidsant, N. Tsubaki, Jet fuel synthesis via Fischer–Tropsch synthesis with varied 1-olefins as additives using Co/ZrO2–SiO2 bimodal catalyst, Fuel 171 (2016) 159–166, https://doi.org/10.1016/j. fuel.2015.12.062.
- [14] J. Li, Y. He, L. Tan, P. Zhang, X. Peng, A. Oruganti, G. Yang, H. Abe, Y. Wang, N. Tsubaki, Integrated tuneable synthesis of liquid fuels via Fischer–Tropsch technology, Nat. Catal. 1 (2018) 787–793, https://doi.org/10.1038/s41929-018-0144-x
- [15] H. Fu, X. Li, S. Shao, Y. Cai, Jet fuel range hydrocarbon generation from catalytic pyrolysis of lignin and polypropylene with iron-modified activated carbon, J. Anal. Appl. Pyrolysis 177 (2024) 106360, https://doi.org/10.1016/j. jaap.2024.106360.
- [16] J. Eilers, S.A. Posthuma, S.T. Sie, The shell middle distillate synthesis process (SMDS), Catal. Lett. 7 (1990) 253–269, https://doi.org/10.1007/BF00764507.
- [17] C. Gomes, Clean Coal as a Transitional Buffer: A Critical Study of Livelihood Strategies Amid South Africa's Energy Decarbonisation. (2025) preprint, http s://doi.org/10.20944/preprints202506.0844.v1, (accessed June 1, 2025).
- [18] A. de Klerk, Fischer-Tropsch fuels refinery design, Energy Environ. Sci. 4 (2011) 1177–1205.
- [19] J. Li, J. Sun, R. Fan, Y. Yoneyama, G. Yang, N. Tsubaki, Selectively converting biomass to jet fuel in Large-scale apparatus, ChemCatChem 9 (2017) 2668–2674, https://doi.org/10.1002/cctc.201700059.
- [20] Clean Energy Technology Observatory, Renewable Fuels of Non-Biological Origin in the European Union. (https://www.h2knowledgecentre.com/content/resea rchpaper6276), 2024 (accessed June 1, 2025).

- [21] thyssenkrupp Uhde selected for Elyse Energy's Biomass-to-SAF project in France. available at: (https://www.thyssenkrupp-uhde.com/en/media/press-releases/ press-detail/thyssenkrupp-uhde-selected-for-elyse-energy)'s-biomass-to-safproject-in-france-296266, 2025 (accessed June 1, 2025).
- [22] C. Bouchy, G. Hastoy, E. Guillon, J.A. Martens, Fischer-Tropsch waxes upgrading via hydrocracking and selective hydroisomerization, Oil Gas. Sci. Technol. Rev. IFP 64 (2009) 91–112, https://doi.org/10.2516/ogst/2008047.
- [23] M.E. Dry, The Fischer–Tropsch process: 1950–2000, Catal. Today (2002) 227–241, https://doi.org/10.1016/S0920-5861(01)00453-9.
- [24] E. Boymans, T. Nijbacker, D. Slort, S. Grootjes, B. Vreugdenhil, Jet fuel synthesis from syngas using bifunctional Cobalt-Based catalysts (1-12), Catalysts 12 (2022) 288, https://doi.org/10.3390/catal12030288.
- [25] S. Sartipi, M. Makkee, F. Kapteijn, J. Gascon, Catalysis engineering of bifunctional solids for the one-step synthesis of liquid fuels from syngas: a review, Catal. Sci. Technol. 4 (2014) 893–907, https://doi.org/10.1039/C3CY01021J.
- [26] J. Bao, J. He, Y. Zhang, Y. Yoneyama, N. Tsubaki, A Core/Shell catalyst produces a spatially confined effect and shape selectivity in a consecutive reaction, Angew. Chem. Int. Ed. 47 (2008) 353–356, https://doi.org/10.1002/anie.200703335.
- [27] Y. Wang, N. Tsubaki, Powerful and new chemical synthesis reactions from CO2 and C1 chemistry innovated by Tailor-Made Core-Shell catalysts, in: H. Yamashita, H. Li (Eds.), Core-Shell Yolk-Shell Nanocatalysts, Springer, Singapore, 2021, pp. 105–120, https://doi.org/10.1007/978-981-16-0463-8.7.
- [28] S. LeViness, S.R. Deshmukh, L.A. Richard, H.J. Robota, Velocys Fischer–Tropsch synthesis Technology—New advances on State-of-the-Art, Top. Catal. 57 (2014) 518–525, https://doi.org/10.1007/s11244-013-0208-x.
- [29] M. Loewert, J. Hoffmann, P. Piermartini, M. Selinsek, R. Dittmeyer, P. Pfeifer, Microstructured Fischer-Tropsch reactor Scale-up and opportunities for decentralized application, Chem. Eng. Technol. 42 (2019) 2202–2214, https://doi.org/10.1002/ceat.201900136.
- [30] R. Myrstad, S. Eri, P. Pfeifer, E. Rytter, A. Holmen, Fischer–Tropsch synthesis in a microstructured reactor, Catal. Today 147 (2009) S301–S304, https://doi.org/ 10.1016/j.cattod.2009.07.011.
- [31] S. Sartipi, M. Alberts, M.J. Meijerink, T.C. Keller, J. Pérez-Ramírez, J. Gascon, F. Kapteijn, Towards liquid fuels from biosyngas: effect of zeolite structure in Hierarchical-Zeolite-Supported cobalt catalysts, ChemSusChem 6 (2013) 1646–1650, https://doi.org/10.1002/cssc.201300339.
- [32] M. Safari, A. Haghtalab, F.A. Roghabadi, Promoting jet fuel production by utilizing a Ru-doped Co-based catalyst of Ru-Co@ c (Zd)@ void@ CeO 2 in fischer tropsch synthesis, RSC Adv. 13 (2023) 35525–35536, https://doi.org/10.1039/ D3RA066241
- [33] J. He, B. Xu, Y. Yoneyama, N. Nishiyama, N. Tsubaki, Designing a new kind of capsule catalyst and its application for direct synthesis of middle isoparaffins from synthesis gas, Chem. Lett. 34 (2005) 148–149, https://doi.org/10.1246/ cl.2005.148.
- [34] C.C. Amoo, C. Xing, N. Tsubaki, J. Sun, Tandem reactions over Zeolite-Based catalysts in syngas conversion, ACS Cent. Sci. 8 (2022) 1047–1062, https://doi. org/10.1021/acscentsci.2c00434.
- [35] S. Sartipi, K. Parashar, M.J. Valero-Romero, V.P. Santos, B. van der Linden, M. Makkee, F. Kapteijn, J. Gascon, Hierarchical H-ZSM-5-supported cobalt for the direct synthesis of gasoline-range hydrocarbons from syngas: advantages, limitations, and mechanistic insight, J. Catal. 305 (2013) 179–190, https://doi. org/10.1016/j.jcat.2013.05.012.
- [36] F.G. Botes, W. Böhringer, The addition of HZSM-5 to the Fischer–Tropsch process for improved gasoline production, Appl. Catal. Gen. 267 (2004) 217–225, https://doi.org/10.1016/j.apcata.2004.03.006.
- [37] Tsubaki Laboratory, (n.d.). (http://www3.u-toyama.ac.jp/tsubaki/eng%20200 7/topics_en.html) (accessed February 12, 2024).
- [38] C.C. Amoo, M. Li, A. Noreen, Y. Fu, E. Maturura, C. Du, R. Yang, X. Gao, C. Xing, N. Tsubaki, Fabricating fe nanoparticles embedded in zeolite y microcrystals as active catalysts for Fischer–Tropsch synthesis, ACS Appl. Nano Mater. 3 (2020) 8096–8103, https://doi.org/10.1021/acsanm.0c01515.
- [39] C.M. Lok, J. Van Doorn, G. Aranda Almansa, Promoted ZSM-5 catalysts for the production of bio-aromatics, a review, Renew. Sustain. Energy Rev. 113 (2019) 109248, https://doi.org/10.1016/j.rser.2019.109248.
- [40] E. Iglesia, Design, synthesis, and use of cobalt-based Fischer-Tropsch synthesis catalysts, Appl. Catal. Gen. 161 (1997) 59–78, https://doi.org/10.1016/S0926-
- [41] E. Iglesia, D. Hibbitts, The Fischer-Tropsch synthesis: a few enduring mechanistic conundrums revisited, J. Catal. 405 (2022) 614–625, https://doi.org/10.1016/j. icat 2021.10.033
- [42] E. Iglesia, S.C. Reyes, R.J. Madon, S.L. Soled, Selectivity control and catalyst design in the Fischer-Tropsch synthesis: sites, pellets, and reactors, in: D.D. Eley, H. Pines, P.B. Weisz (Eds.), Adv. Catal, Academic Press, 1993, pp. 221–302, https://doi.org/10.1016/S0360-0564(08)60579-9.
- [43] G.P. Van Der Laan, A. Beenackers, Kinetics and selectivity of the Fischer–Tropsch synthesis: a literature review, Catal. Rev. 41 (1999) 255–318, https://doi.org/ 10.1081/CR-100101170.
- [44] A. Mena Subiranas, G. Schaub, Combining Fischer-Tropsch (FT) and hydrocarbon reactions under FT reaction conditions: model compound and combined-catalyst studies, Int. J. Chem. React. Eng. 7 (2009).
- [45] A.N. Pour, M. Zare, S.M. Kamali Shahri, Y. Zamani, M.R. Alaei, Catalytic behaviors of bifunctional Fe-HZSM-5 catalyst in Fischer–Tropsch synthesis, J. Nat. Gas. Sci. Eng. 1 (2009) 183–189, https://doi.org/10.1016/j. jngse.2009.11.003.
- [46] A. Freitez, K. Pabst, B. Kraushaar-Czarnetzki, G. Schaub, Single-Stage Fischer-Tropsch synthesis and hydroprocessing: the hydroprocessing

- performance of Ni/ZSM-5/ γ -Al2O3 under Fischer–Tropsch conditions, Ind. Eng. Chem. Res. 50 (2011) 13732–13741, https://doi.org/10.1021/ie201913s.
- [47] Q. Cheng, Y. Tian, S. Lyu, N. Zhao, K. Ma, T. Ding, Z. Jiang, L. Wang, J. Zhang, L. Zheng, F. Gao, L. Dong, N. Tsubaki, X. Li, Confined small-sized cobalt catalysts stimulate carbon-chain growth reversely by modifying ASF law of Fischer–Tropsch synthesis, Nat. Commun. 9 (2018) 3250, https://doi.org/10.1038/s41467-018-05755-8.
- [48] H.M. Torres Galvis, K.P. de Jong, Catalysts for production of lower olefins from synthesis gas: a review, ACS Catal. 3 (2013) 2130–2149, https://doi.org/ 10.1021/cs4003436.
- [49] Longya Xu, Qingxia Wang, Yide Xu, Jiasheng Huang, Promotion effect of K2O and MnO additives on the selective production of light alkenes via syngas over Fe/ silicalite-2 catalysts, Catal. Lett. 31 (1995) 253–266, https://doi.org/10.1007/ BF00808838.
- [50] H.M. Torres Galvis, J.H. Bitter, C.B. Khare, M. Ruitenbeek, A.I. Dugulan, K.P. de Jong, Supported iron nanoparticles as catalysts for sustainable production of lower olefins, Science 335 (2012) 835–838, https://doi.org/10.1126/ science 1215614
- [51] H.M.T. Galvis, A.C. Koeken, J.H. Bitter, T. Davidian, M. Ruitenbeek, A.I. Dugulan, K.P. de Jong, Effects of sodium and sulfur on catalytic performance of supported iron catalysts for the Fischer–Tropsch synthesis of lower olefins, J. Catal. 303 (2013) 22–30, https://doi.org/10.1016/j.jcat.2013.03.010.
- [52] H.M.T. Galvis, A.C. Koeken, J.H. Bitter, T. Davidian, M. Ruitenbeek, A.I. Dugulan, K.P. de Jong, Effect of precursor on the catalytic performance of supported iron catalysts for the Fischer–Tropsch synthesis of lower olefins, Catal. Today 215 (2013) 95–102, https://doi.org/10.1016/j.cattod.2013.03.018.
- [53] H. Yu, C. Wang, T. Lin, Y. An, Y. Wang, Q. Chang, F. Yu, Y. Wei, F. Sun, Z. Jiang, S. Li, Y. Sun, L. Zhong, Direct production of olefins from syngas with ultrahigh carbon efficiency, Nat. Commun. 13 (2022) 5987, https://doi.org/10.1038/s41467-022-33715-w.
- [54] D. Zhao, Z. Wang, S. Lyu, Y. Liu, S. Xiong, Y. Zhang, Y. Pan, Q. Cheng, X. Li, Namanipulated reaction pathways boosting long-chain olefin production via Fischer-Tropsch synthesis over NaRu/TiO2 catalysts, Appl. Catal. B Environ. Energy 377 (2025) 125469, https://doi.org/10.1016/j.apcatb.2025.125469.
- [55] A.-H. Nasser, L. Guo, H. ELnaggar, Y. Wang, X. Guo, A. AbdelMoneim, N. Tsubaki, Mn–Fe nanoparticles on a reduced graphene oxide catalyst for enhanced olefin production from syngas in a slurry reactor, RSC Adv. 8 (2018) 14854–14863, https://doi.org/10.1039/CSRA02193G.
- [56] E. Hondo, P. Lu, P. Zhang, J. Li, N. Tsubaki, Direct production of hydrocarbons by Fischer-Tropsch synthesis using newly designed catalysts, J. Jpn. Pet. Inst. 63 (2020) 239–247, https://doi.org/10.1627/jpi.63.239.
- [57] G. Liu, Q. Chen, E. Oyunkhand, S. Ding, N. Yamane, G. Yang, Y. Yoneyama, N. Tsubaki, Nitrogen-rich mesoporous carbon supported iron catalyst with superior activity for Fischer-Tropsch synthesis, Carbon 130 (2018) 304–314, https://doi.org/10.1016/j.carbon.2018.01.015.
- [58] M.-L. Zhu, X. Liu, Y. Niu, G.-Q. Yang, J. Bao, Y.-H. Song, Y.-F. Yan, N. Du, M.-L. Shui, K. Zhu, B. Zhang, Z.-T. Liu, D. Ma, Z.-W. Liu, Long-chain α-olefins production over Co-MnOx catalyst with optimized interface, Appl. Catal. B Environ. Energy 346 (2024) 123783, https://doi.org/10.1016/j.apcath.2024.123783
- [59] L. Zhong, F. Yu, Y. An, Y. Zhao, Y. Sun, Z. Li, T. Lin, Y. Lin, X. Qi, Y. Dai, Cobalt carbide nanoprisms for direct production of lower olefins from syngas, Nature 538 (2016) 84–87, https://doi.org/10.1038/nature19786.
- [60] L. Tan, F. Wang, P. Zhang, Y. Suzuki, Y. Wu, J. Chen, G. Yang, N. Tsubaki, Design of a core-shell catalyst: an effective strategy for suppressing side reactions in syngas for direct selective conversion to light olefins, Chem. Sci. 11 (2020) 4097–4105, https://doi.org/10.1039/C9SC05544D.
- [61] F. Jiao, J. Li, X. Pan, J. Xiao, H. Li, H. Ma, M. Wei, Y. Pan, Z. Zhou, M. Li, S. Miao, J. Li, Y. Zhu, D. Xiao, T. He, J. Yang, F. Qi, Q. Fu, X. Bao, Selective conversion of syngas to light olefins, Science 351 (2016) 1065–1068, https://doi.org/10.1126/science.aaf1835.
- [62] K. Cheng, B. Gu, X. Liu, J. Kang, Q. Zhang, Y. Wang, Direct and highly selective conversion of synthesis gas into lower olefins: design of a bifunctional catalyst combining methanol synthesis and Carbon–Carbon coupling, Angew. Chem. Int. Ed. 55 (2016) 4725–4728, https://doi.org/10.1002/anie.201601208.
- [63] N.C. Shiba, X. Liu, Y. Yao, Advances in lower olefin production over cobalt-based catalysts via the Fischer-Tropsch process, Fuel Process. Technol. 238 (2022) 107489, https://doi.org/10.1016/j.fuproc.2022.107489.
- [64] W. Gong, R.-P. Ye, J. Ding, T. Wang, X. Shi, C.K. Russell, J. Tang, E.G. Eddings, Y. Zhang, M. Fan, Effect of copper on highly effective Fe-Mn based catalysts during production of light olefins via Fischer-Tropsch process with low CO2 emission, Appl. Catal. B Environ. 278 (2020) 119302, https://doi.org/10.1016/j.apcath.2020.119302
- [65] Y. Chen, Y. Xu, D. Cheng, Y. Chen, F. Chen, X. Lu, Y. Huang, S. Ni, Synthesis of CuO–ZnO–Al2O3 @ SAPO-34 core@shell structured catalyst by intermediate layer method, Pure Appl. Chem. 86 (2014) 775–783, https://doi.org/10.1515/ pac-2013-1121.
- [66] G. Yang, F. Meng, P. Zhang, L. Yang, Z. Li, Effects of preparation method and precipitant on Mn–Ga oxide in combination with SAPO-34 for syngas conversion into light olefins, N. J. Chem. 45 (2021) 7967–7976, https://doi.org/10.1039/ D1N 100443C
- [67] F. Meng, X. Li, P. Zhang, L. Yang, G. Yang, P. Ma, Z. Li, Highly active ternary oxide ZrCeZnOx combined with SAPO-34 zeolite for direct conversion of syngas into light olefins, Catal. Convers. Low. Carbon Sustain. Resour. 368 (2021) 118–125, https://doi.org/10.1016/j.cattod.2020.03.023.

- [68] P. Zhang, F. Meng, L. Yang, G. Yang, X. Liang, Z. Li, Syngas to olefins over a CrMnGa/SAPO-34 bifunctional catalyst: effect of cr and Cr/Mn ratio, Ind. Eng. Chem. Res. 60 (2021) 13214–13222, https://doi.org/10.1021/acs.iecr.1c02150.
- [69] Verkehrswende and PtX Hub, Analysis: Defossilising aviation with e-SAF-An introduction to technologies, policies, and markets for, https://www.agora-verkehrswende.de/fileadmin/Projekte/2024/E-Fuels-im-Luftverkehr_EN/111_Defossilising_Aviation_with_e-SAF.pdf), 2024 (accessed August 13, 2025).
- [70] K. Ramasamy, Syngas Derived Mixed Olefin Oligomerization for Sustainable Aviation Fuel-Pacific Northwest National Laboratory. (https://www.energy.gov/sites/default/files/2023-04/beto-16-project-peer-review-cat-apr-2023-ramasamy.pdf), 2023 (accessed August 13, 2025).
- [71] Powering the future of air travel with sustainable aviation fuel (www.metafuels.ch), (n.d.). (https://indico.psi.ch/event/12715/attachments/21172/46564/06_2023_Metafuels_Energy_Briefing_Bern_Rev1_final.pdf), 2023 (accessed August 13, 2025)
- [72] From CO2 and H2 to Sustainable Aviation Fuel TAKE-OFF. (https://papers.ssm.com/sol3/papers.cfm?abstract_id=5016154), 2024 (accessed August 13, 2025).
- [73] C. Fuchs, U. Arnold, J. Sauer, Synthesis of sustainable aviation fuels via (co–) oligomerization of light olefins, Fuel 382 (2025) 133680, https://doi.org/ 10.1016/j.fuel.2024.133680.
- [74] C. Fuchs, U. Arnold, J. Sauer, Co-)Oligomerization of olefins to hydrocarbon fuels: influence of feed composition and pressure, Chem. Ing. Tech. 95 (2023) 651–657, https://doi.org/10.1002/cite.202200209.
- [75] S.S. Iyer, T. Renganathan, S. Pushpavanam, M. Vasudeva Kumar, N. Kaisare, Generalized thermodynamic analysis of methanol synthesis: effect of feed composition, J. CO2 Util. 10 (2015) 95–104, https://doi.org/10.1016/j. icou.2015.01.006.
- [76] V. Dieterich, A. Buttler, A. Hanel, H. Spliethoff, S. Fendt, Power-to-liquid via synthesis of methanol, DME or Fischer–Tropsch-fuels: a review, Energy Environ. Sci. 13 (2020) 3207–3252, https://doi.org/10.1039/D0EE01187H.
- [77] A. Elwalily, E. Verkama, F. Mantei, A. Kaliyeva, A. Pounder, J. Sauer, F. Nestler, Sustainable aviation fuel production via the methanol pathway: a technical review, Sustain. Energy Fuels (2025), https://doi.org/10.1039/D5SE00231A.
- [78] H. Shi, J. Peng, X. Cheng, X. Yang, J. Jin, J. Hu, The CO2 desorption analysis of tri-solvent MEA+BEA+DEEA with several commercial solid acid catalysts, Int. J. Greenh. Gas. Control 116 (2022) 103647, https://doi.org/10.1016/j. ijggc.2022.103647.
- [79] J. Van Kampen, J. Boon, J. Vente, M. van Sint Annaland, Sorption enhanced dimethyl ether synthesis under industrially relevant conditions: experimental validation of pressure swing regeneration, React. Chem. Eng. 6 (2021) 244–257, https://doi.org/10.1039/D0RE00431F.
- [80] J. Van Kampen, J. Boon, J. Vente, M. van Sint Annaland, Sorption enhanced dimethyl ether synthesis for high efficiency carbon conversion: modelling and cycle design, J. CO2 Util. 37 (2020) 295–308, https://doi.org/10.1016/j. icou.2019.12.021.
- [81] J. Terreni, M. Trottmann, T. Franken, A. Heel, A. Borgschulte, Sorption-enhanced methanol synthesis, Energy Technol. 7 (2019) 1801093, https://doi.org/ 10.1002/ente.201801093.
- [82] F. Dalena, A. Senatore, M. Basile, S. Knani, A. Basile, A. Iulianelli, Advances in methanol production and utilization, with particular emphasis toward hydrogen generation via membrane reactor technology, Membranes 8 (2018) 98, https:// doi.org/10.3390/membranes8040098.
- [83] M.R. Rahimpour, M. Lotfinejad, Co-current and countercurrent configurations for a membrane dual type methanol reactor, Chem. Eng. Technol. 31 (2008) 38–57, https://doi.org/10.1002/ceat.200700269.
- [84] MTJetTM Technology, (https://www.topsoe.com/our-resources/knowledge/our-products/process-licensing/mtjet-process), 2025 (accessed August 13, 2025).
- [85] ExxonMobil. (2022, June 20). ExxonMobil methanol to jet technology to provide new route for sustainable aviation fuel production. (https://www.exxonmobil lchemical.com/-/media/media-assets/media-library-assets/17/exxonmobil sustainable_aviation_fuel_production_en.pdf/ (accessed August 13, 2025).
- [86] S.J. McCarthy, B.J. O'neill, Integrated oxygenate conversion and olefin oligomerization, US10590353B2, 2020. https://patents.google.com/patent/ /US10590353B2/en/, (accessed August 22, 2025).
- [87] P. Beato-Haldor Topsøe A/S, Methanol to Jet Fuel (MTJ) Process. WO2022/063994 A1, 2022. (https://patents.google.com/patent/WO2022063994A1/en), (accessed August 22, 2025).
- [88] N.C. Schjødt, P. Beato, F. Joensen, R.Y. Brogaard, L.E. Sommer, Process and plant for conversion of oxygenates, WO2023138876A1, 2025. (https://patents.google. com/patent/EP4466328A1/en), (accessed August 22, 2025).
- [89] C. Perego, G.F. Rispoli, Process for producing fuels from waste by converting olefins from methanol, WO2025022352A1, 2025. ⟨https://patents.google.com/p atent/WO2025022352A1/en⟩ (accessed August 22, 2025).
- [90] C. Perego, G.F. Rispoli, Process for producing fuels from waste by converting olefins from methanol to propylene (mtp), WO2025022348A1, 2025. (https://pa ents.google.com/patent/WO2025022348A1/en) (accessed August 22, 2025).
- [91] J. Zhou, M. Gao, J. Zhang, W. Liu, T. Zhang, H. Li, Z. Xu, M. Ye, Z. Liu, Directed transforming of coke to active intermediates in methanol-to-olefins catalyst to boost light olefins selectivity, Nat. Commun. 12 (2021) 17, https://doi.org/ 10.1038/s41467-020-20193-1.
- [92] L. Yang, C. Wang, L. Zhang, W. Dai, Y. Chu, J. Xu, G. Wu, M. Gao, W. Liu, Z. Xu, P. Wang, N. Guan, M. Dyballa, M. Ye, F. Deng, W. Fan, L. Li, Stabilizing the framework of SAPO-34 zeolite toward long-term methanol-to-olefins conversion, Nat. Commun. 12 (2021) 4661, https://doi.org/10.1038/s41467-021-24403-2.
- [93] Y. Zhou, S. Santos, M. Shamzhy, M. Marinova, A.-M. Blanchenet, Y.G. Kolyagin, P. Simon, M. Trentesaux, S. Sharna, O. Ersen, V.L. Zholobenko, M. Saeys, A.

- Y. Khodakov, V.V. Ordomsky, Liquid metals for boosting stability of zeolite catalysts in the conversion of methanol to hydrocarbons, Nat. Commun. 15 (2024) 2228, https://doi.org/10.1038/s41467-024-46232-9.
- [94] I.B. Minova, N.S. Barrow, A.C. Sauerwein, A.B. Naden, D.B. Cordes, A.M. Z. Slawin, S.J. Schuyten, P.A. Wright, Silicon redistribution, acid site loss and the formation of a core–shell texture upon steaming SAPO-34 and their impact on catalytic performance in the Methanol-to-Olefins (MTO) reaction, J. Catal. 395 (2021) 425–444, https://doi.org/10.1016/j.jcat.2021.01.012.
- [95] S. Zhang, Y. Gong, L. Zhang, Y. Liu, T. Dou, J. Xu, F. Deng, Hydrothermal treatment on ZSM-5 extrudates catalyst for methanol to propylene reaction: finely tuning the acidic property, Fuel Process. Technol. 129 (2015) 130–138, https:// doi.org/10.1016/j.fuproc.2014.09.006.
- [96] L. Zhang, R. Tu, G. Ren, Z. Li, S. Zhai, Y. Xu, T. Yu, Manipulate the acidity of gallium doped Silicalite-1 to optimize methanol to propene performance, Chem. Eng. J. 458 (2023) 141447, https://doi.org/10.1016/j.cej.2023.141447.
- [97] F.H. Alshafei, S.I. Zones, M.E. Davis, Improving the propylene selectivity in the methanol-to-olefins reaction over CIT-17, a SAT-type molecular sieve, Chem. Eng. J. 482 (2024) 149045, https://doi.org/10.1016/j.cej.2024.149045.
- [98] G.C. Chinchen, P.J. Denny, J.R. Jennings, M.S. Spencer, K.C. Waugh, Synthesis of methanol: part 1. Catalysts and kinetics, Appl. Catal. 36 (1988) 1–65, https://doi. org/10.1016/S0166-9834(00)80103-7.
- [99] F. Chen, W. Gao, K. Wang, C. Wang, X. Wu, N. Liu, X. Guo, Y. He, P. Zhang, G. Yang, N. Tsubaki, Enhanced performance and stability of Cu/ZnO catalyst by introducing MgO for low-temperature methanol synthesis using methanol itself as catalytic promoter, Fuel 315 (2022) 123272, https://doi.org/10.1016/j.fipel_2022_133272
- [100] O. Martin, A.J. Martín, C. Mondelli, S. Mitchell, T.F. Segawa, R. Hauert, C. Drouilly, D. Curulla-Ferré, J. Pérez-Ramírez, Indium oxide as a superior catalyst for methanol synthesis by CO2 hydrogenation, Angew. Chem. 128 (2016) 6369–6373, https://doi.org/10.1002/ange.201600943.
- [101] E. Frei, A. Schaadt, T. Ludwig, H. Hillebrecht, I. Krossing, The influence of the Precipitation/Ageing temperature on a Cu/ZnO/ZrO2 catalyst for methanol synthesis from H2 and CO2, ChemCatChem 6 (2014) 1721–1730, https://doi.org/ 10.1002/cctc.201300665.
- [102] J. Kang, S. He, W. Zhou, Z. Shen, Y. Li, M. Chen, Q. Zhang, Y. Wang, Single-pass transformation of syngas into ethanol with high selectivity by triple tandem catalysis, Nat. Commun. 11 (2020), https://doi.org/10.1038/s41467-020-14672-8
- [103] M.R. Gogate, R.J. Davis, X-ray absorption spectroscopy of an Fe-promoted Rh/ TiO2 catalyst for synthesis of ethanol from synthesis gas, ChemCatChem 1 (2009) 295–303, https://doi.org/10.1002/cctc.200900104.
- [104] T. Han, L. Zhao, G. Liu, H. Ning, Y. Yue, Y. Liu, Rh-Fe alloy derived from YRh0.5Fe0.5O3/ZrO2 for higher alcohols synthesis from syngas, Catal. Today 298 (2017) 69–76, https://doi.org/10.1016/j.cattod.2017.05.057.
- [105] W. Liu, S. Wang, T. Sun, S. Wang, The promoting effect of fe doping on Rh/CeO2 for the ethanol synthesis, Catal. Lett. 145 (2015) 1741–1749, https://doi.org/10.1007/s10562-015-1577-5.
- [106] Y. Liu, F. Göeltl, I. Ro, M.R. Ball, C. Sener, I.B. Aragão, D. Zanchet, G.W. Huber, M. Mavrikakis, J.A. Dumesic, Synthesis gas conversion over Rh-Based catalysts promoted by fe and mn, ACS Catal. 7 (2017) 4550–4563, https://doi.org/ 10.1021/acscatal.7b01381.
- [107] M.A. Haider, M.R. Gogate, R.J. Davis, Fe-promotion of supported rh catalysts for direct conversion of syngas to ethanol, J. Catal. 261 (2009) 9–16, https://doi.org/ 10.1016/j.jcat.2008.10.013.
- [108] C. Wang, J. Zhang, G. Qin, L. Wang, E. Zuidema, Q. Yang, S. Dang, C. Yang, J. Xiao, X. Meng, C. Mesters, F.S. Xiao, Direct conversion of syngas to ethanol within zeolite crystals, Chem 6 (2020) 646–657, https://doi.org/10.1016/j. chempr.2019.12.007.
- [109] D. Ferrari, G. Budroni, L. Bisson, N.J. Rane, B.D. Dickie, J.H. Kang, S.J. Rozeveld, Effect of potassium addition method on MoS2 performance for the syngas to alcohol reaction, Appl. Catal. Gen. 462–463 (2013) 302–309, https://doi.org/ 10.1016/j.apcata.2013.05.006.
- [110] N. Wang, J. Li, R. Hu, Y. Zhang, H. Su, X. Gu, Enhanced catalytic performance and promotional effect of molybdenum sulfide cluster-derived catalysts for higher alcohols synthesis from syngas, Catal. Today 316 (2018) 177–184, https://doi. org/10.1016/j.cattod.2018.03.007.
- [111] S. Guo, S. Li, H. Zhong, D. Gong, J. Wang, N. Kang, L. Zhang, G. Liu, Y. Liu, Mixed oxides confined and tailored cobalt nanocatalyst for direct ethanol synthesis from syngas: a catalyst designing by using Perovskite-Type oxide as the precursor, Ind. Eng. Chem. Res. 57 (2018) 2404–2415, https://doi.org/10.1021/acs.iogr/7b04336
- [112] J. Wang, G. Liu, H. Zhong, P. Song, K. An, Z. Zhang, A. Cao, Y. Liu, In situ topochemical carbonization derivative Co-Ni alloy@Co-Co2C for direct ethanol synthesis from syngas, Appl. Surf. Sci. 557 (2021), https://doi.org/10.1016/j. apsusc.2021.149826.
- [113] K. Sun, M. Tan, Y. Bai, X. Gao, P. Wang, N. Gong, T. Zhang, G. Yang, Y. Tan, Design and synthesis of spherical-platelike ternary copper-cobalt-manganese catalysts for direct conversion of syngas to ethanol and higher alcohols, J. Catal. 378 (2019) 1–16, https://doi.org/10.1016/j.jcat.2019.08.013.
- [114] Y. Hao, D. Zhao, Y. Zhou, M. Yin, Z. Wang, G. Xi, S. Song, Q. Tang, J.H. Yang, Hierarchical leaf-like alumina-carbon nanosheets with ammonia water modification for ethanol dehydration to ethylene, Fuel 333 (2023), https://doi. org/10.1016/j.fuel.2022.126128.
- [115] E. Quiroga, N. García, B. Cifuentes, R. Cogua, J. Becerra, J.M. Berenguer, M. Cobo, Industrial crude bioethanol dehydration to ethylene: doping ZSM-5 to

- enhance selectivity and stability, 111803-111803, J. Environ. Chem. Eng. (2023), https://doi.org/10.1016/j.jece.2023.111803.
- [116] M. Florea, A. Bocirnea, S. Neaţu, A.M. Kuncser, M.M. Trandafir, F. Neaţu, Tuning the acidity by addition of transition metal to mn modified hollow silica spheres and their catalytic activity in ethanol dehydration to ethylene, Appl. Catal. Gen. 646 (2022), https://doi.org/10.1016/j.apcata.2022.118860.
- [117] S. Andreoli, C. Oldani, V. Fiorini, S. Stagni, G. Fornasari, S. Albonetti, Superacid Aquivion® PFSA as an efficient catalyst for the gas phase dehydration of ethanol to ethylene in mild conditions, Appl. Catal. Gen. 597 (2020), https://doi.org/ 10.1016/j.apcata.2020.117544.
- [118] Y.W. Cheng, C.C. Chong, C.K. Cheng, K.H. Ng, T. Witoon, J.C. Juan, Ethylene production from ethanol dehydration over mesoporous SBA-15 catalyst derived from palm oil clinker waste, J. Clean. Prod. 249 (2020), https://doi.org/10.1016/ j.jclepro.2019.119323.
- [119] P. Trongjitraksa, Y. Klinthongchai, P. Praserthdam, B. Jongsomjit, Elucidation on supporting effect of WO3 over MCF-Si and SBA-15 catalysts toward thanol dehydration, J. Taiwan Inst. Chem. Eng. 152 (2023), https://doi.org/10.1016/j. jtice.2023.105168.
- [120] G. Liu, G. Yang, X. Peng, J. Wu, N. Tsubaki, Recent advances in the routes and catalysts for ethanol synthesis from syngas, Chem. Soc. Rev. 51 (2022) 5606–5659, https://doi.org/10.1039/d0cs01003k.
- [121] P. Mäki-Arvela, A. Aho, I. Simakova, D. Yu. Murzin, Sustainable aviation fuel from syngas through higher alcohols, ChemCatChem 14 (2022) e202201005, https://doi.org/10.1002/cctc.202201005.
- [122] P. Preikschas, J. Bauer, K. Knemeyer, R. Naumann D'Alnoncourt, R. Kraehnert, F. Rosowski, Formation, dynamics, and long-term stability of Mn- and Fepromoted Rh/SiO2catalysts in CO hydrogenation, Catal. Sci. Technol. 11 (2021) 5802–5815, https://doi.org/10.1039/d1cy00421b.
- [123] D. Damma, T. Boningari, P.G. Smirniotis, Multimetallic Rh-La/M/SiO2 (M = W, V, Ce, and Zr) catalysts for oxygenates synthesis from syngas, Chem. Eng. Sci. 243 (2021), https://doi.org/10.1016/j.ces.2021.116778.
- [124] J. Liu, Z. Guo, D. Childers, N. Schweitzer, C.L. Marshall, R.F. Klie, J.T. Miller, R. J. Meyer, Correlating the degree of metal-promoter interaction to ethanol selectivity over MnRh/CNTs CO hydrogenation catalysts, J. Catal. 313 (2014) 149–158, https://doi.org/10.1016/j.jcat.2014.03.002.
- [125] X. Pan, Z. Fan, W. Chen, Y. Ding, H. Luo, X. Bao, Enhanced ethanol production inside carbon-nanotube reactors containing catalytic particles, Nat. Mater. 6 (2007) 507–511, https://doi.org/10.1038/nmat1916.
- [126] J. Sun, S. Wan, F. Wang, J. Lin, Y. Wang, Selective synthesis of methanol and higher alcohols over Cs/Cu/ZnO/Al2O3 catalysts, Ind. Eng. Chem. Res. 54 (2015) 7841–7851, https://doi.org/10.1021/acs.iecr.5b01927.
- [127] H.T. Luk, C. Mondelli, D.C. Ferré, J.A. Stewart, J. Pérez-Ramírez, Status and prospects in higher alcohols synthesis from syngas, Chem. Soc. Rev. 46 (2017) 1358–1426, https://doi.org/10.1039/c6cs00324a.
- [128] S. Xie, Z. Li, S. Luo, W. Zhang, Bioethanol to jet fuel: current status, challenges, and perspectives, Renew. Sustain. Energy Rev. 192 (2024), https://doi.org/ 10.1016/j.rser.2023.114240.
- [129] L. Ouayloul, M. El Doukkali, M. Jiao, F. Dumeignil, I. Agirrezabal-Telleria, New mechanistic insights into the role of water in the dehydration of ethanol into ethylene over ZSM-5 catalysts at low temperature, Green. Chem. 25 (2023) 3644–3659, https://doi.org/10.1039/d2gc04437d.
- [130] C.Y. Wu, H.S. Wu, Ethylene formation from ethanol dehydration using ZSM-5 catalyst, ACS Omega 2 (2017) 4287–4296, https://doi.org/10.1021/ acsomega.7b00680.
- [131] D. Masih, S. Rohani, J.N. Kondo, T. Tatsumi, Catalytic dehydration of ethanol-toethylene over rho zeolite under mild reaction conditions, Microporous Mesoporous Mater. 282 (2019) 91–99, https://doi.org/10.1016/j. micromeso 2019 01 035
- [132] A. Styskalik, V. Vykoukal, L. Fusaro, C. Aprile, D.P. Debecker, Mildly acidic aluminosilicate catalysts for stable performance in ethanol dehydration, Appl. Catal. B Environ. 271 (2020), https://doi.org/10.1016/j.apcatb.2020.118926.
- [133] R. Henry, M. Komurcu, Y. Ganjkhanlou, R.Y. Brogaard, L. Lu, K.-J. Jens, G. Berlier, U. Olsbye, Ethene oligomerization on nickel microporous and mesoporous-supported catalysts: investigation of the active sites, Catal. Today 299 (2018) 154–163.
- [134] C.P. Nicholas, Applications of light olefin oligomerization to the production of fuels and chemicals, Appl. Catal. Gen. 543 (2017) 82–97, https://doi.org/ 10.1016/j.apcata.2017.06.011.
- [135] R.Y. Brogaard, M. Kømurcu, M.M. Dyballa, A. Botan, V. Van Speybroeck, U. Olsbye, K. De Wispelaere, Ethene dimerization on zeolite-hosted ni ions: reversible mobilization of the active site, ACS Catal. 9 (2019) 5645–5650.
- [136] C.M. Halmenschlager, M. Brar, I.T. Apan, A. de Klerk, Oligomerization of Fischer–Tropsch tail gas over H-ZSM-5, Ind. Eng. Chem. Res. 55 (2016) 13020–13031, https://doi.org/10.1021/acs.iecr.6b03861.
- [137] A. de Klerk, Effect of oxygenates on the oligomerization of Fischer—Tropsch olefins over amorphous Silica—Alumina, Energy Fuels 21 (2007) 625–632, https://doi.org/10.1021/ef060485y.
- [138] F.J. Dubray, V. Paunovic, J.A. Van Bokhoven, Optimization of sustainable aviation fuel production through Experiment-Driven modeling of Acid-Catalyzed oligomerization, ACS Sustain. Chem. Eng. 12 (2024) 17590–17599, https://doi. org/10.1021/acssuschemeng.4c08240.
- [139] F. Dubray, V. Paunović, M. Ranocchiari, J.A. van Bokhoven, Production of jet-fuel-range olefins via catalytic conversion of pentene and hexene over mesoporous Al-SBA-15 catalyst, J. Ind. Eng. Chem. 114 (2022) 409–417, https://doi.org/10.1016/j.jiec.2022.07.030.

- [140] A. de Klerk, Properties of synthetic fuels from H-ZSM-5 oligomerization of Fischer–Tropsch type feed materials, Energy Fuels 21 (2007) 3084–3089, https://doi.org/10.1021/ef700246k.
- [141] M. Betz, C. Fuchs, T.A. Zevaco, U. Arnold, J. Sauer, Production of hydrocarbon fuels by heterogeneously catalyzed oligomerization of ethylene: tuning of the product distribution, Biomass.. Bioenergy 166 (2022) 106595, https://doi.org/ 10.1016/j.biombioe.2022.106595.
- [142] M.H. Kwon, J.S. Yoon, M. Lee, D.W. Hwang, Y. Kim, M.B. Park, H.J. Chae, One-pot cascade ethylene oligomerization using Ni/Siral-30 and H-ZSM-5 catalysts, Appl. Catal. Gen. 572 (2019) 226–231, https://doi.org/10.1016/j.apcata.2018.12.005.
- [143] M. Lee, J.W. Yoon, Y. Kim, J.S. Yoon, H.J. Chae, Y.H. Han, D.W. Hwang, Ni/ SIRAL-30 as a heterogeneous catalyst for ethylene oligomerization, Appl. Catal. Gen. 562 (2018) 87–93, https://doi.org/10.1016/j.apcata.2018.06.004.
- [144] S. Moon, H.J. Chae, M.B. Park, Oligomerization of light olefins over ZSM-5 and beta zeolite catalysts by modifying textural properties, Appl. Catal. Gen. 553 (2018) 15–23, https://doi.org/10.1016/j.apcata.2018.01.015.
- [145] P. Panpian, T.T.V. Tran, S. Kongparakul, L. Attanatho, Y. Thanmongkhon, P. Wang, G. Guan, N. Chanlek, Y. Poo-arporn, C. Samart, Production of bio-jet fuel through ethylene oligomerization using NiAlKIT-6 as a highly efficient catalyst, Fuel 287 (2021), https://doi.org/10.1016/j.fuel.2020.119831.
- [146] Q. Zhang, T. Wang, Y. Li, R. Xiao, T. Vitidsant, P. Reubroycharoen, C. Wang, Q. Zhang, L. Ma, Olefin-rich gasoline-range hydrocarbons from oligomerization of bio-syngas over Ni/ASA catalyst, Fuel Process. Technol. 167 (2017) 702–710, https://doi.org/10.1016/j.fuproc.2017.07.035.
- [147] B.H. Babu, M. Lee, D.W. Hwang, Y. Kim, H.-J. Chae, An integrated process for production of jet-fuel range olefins from ethylene using Ni-AlSBA-15 and Amberlyst-35 catalysts, Appl. Catal. Gen. 530 (2017) 48–55, https://doi.org/ 10.1016/j.apcata.2016.11.020.
- [148] H.O. Mohamed, O. Abed, N. Zambrano, P. Castaño, I. Hita, A Zeolite-Based cascade system to produce jet fuel from ethylene oligomerization, Ind. Eng. Chem. Res. 61 (2022) 15880–15892, https://doi.org/10.1021/acs.iecr.2c02303.

- [149] W. Keim, Oligomerization of ethylene to α-Olefins: discovery and development of the shell higher olefin process (SHOP), Angew. Chem. Int. Ed. 52 (2013) 12492–12496, https://doi.org/10.1002/anie.201305308.
- [150] Sustainable Aviation Business Overview-Honeywell, (https://process.honeywell. com/content/dam/process/en/documents/document-lists/Sustainable-Aviation -Business-Overview.pdf), 2023 (accessed June 1, 2025).
- [151] C.P. Nicholas, A. Bhattacharyya, D.E. Mackowiak, Process for oligomerizing dilute ethylene, US8748681B2, 2014. (https://patents.google.com/patent /US8748681B2/en) (accessed June 19, 2025).
- [152] N.M. Eagan, M.D. Kumbhalkar, J.S. Buchanan, J.A. Dumesic, G.W. Huber, Chemistries and processes for the conversion of ethanol into middle-distillate fuels, Nat. Rev. Chem. 3 (2019) 223–249, https://doi.org/10.1038/s41570-019-0084-4
- [153] A. Jonathan, E.G. Tomashek, M.P. Lanci, J.A. Dumesic, G.W. Huber, Reaction kinetics study of ethylene oligomerization into linear olefins over carbonsupported cobalt catalysts, J. Catal. 404 (2021) 954–963, https://doi.org/ 10.1016/j.jcat.2021.05.035.
- [154] A. Martínez Gómez-Aldaraví, C. Paris, M. Moliner, C. Martínez, Design of bifunctional Ni-zeolites for ethylene oligomerization: controlling ni speciation and zeolite properties by one-pot and post-synthetic ni incorporation, J. Catal. 426 (2023) 140–152, https://doi.org/10.1016/j.jcat.2023.07.010.
- [155] L. Attanatho, S. Lao-ubol, A. Suemanotham, N. Prasongthum, P. Khowattana, T. Laosombut, N. Duangwongsa, S. Larpkiattaworn, Y. Thanmongkhon, Jet fuel range hydrocarbon synthesis through ethylene oligomerization over platelet Ni-AlSBA-15 catalyst, SN Appl. Sci. 2 (2020), https://doi.org/10.1007/s42452-020-2784-2
- [156] J.A. Okolie, D. Awotoye, M.E. Tabat, P.U. Okoye, E.I. Epelle, C.C. Ogbaga, F. Güleç, B. Oboirien, Multi-criteria decision analysis for the evaluation and screening of sustainable aviation fuel production pathways, iScience 26 (2023) 106944, https://doi.org/10.1016/j.isci.2023.106944.